Magazine of Civil Engineering

ISSN 2712-8172

journal homepage: http://engstroy.spbstu.ru/

DOI: 10.34910/MCE.110.7

Application of artificial neural networks for prediction of concrete properties

N.A. Abdulla
University of Salahaddin, Erbil, Iraq
E-mail: anwzad@yahoo.com

Keywords: slump, aggregate/cement ratio, artificial neural network, concrete stress, strain at peak stress, regression analysis

Abstract. The effect of different mix ratios on the mechanical properties of concrete was investigated. The strength and deformation in terms of the strain of normal strength concrete were evaluated under concentric loading. The artificial neural network (ANN) technique was used for predicting the compressive stress and strain at peak stress of concrete. The input parameters for ANN architectures included water/cement ratio, aggregate/cement ratio, and slump values. An equation for predicting the strain of concrete at peak stress was proposed based on ANN output values for compressive stress and strain at peak stress. The capability and performance of the proposed equation are compared with actual experimental results and predictions from existing fifty-three empirical equations, including several design codes and various strain models for normal and high strength concretes, using several statistical indexes. The results showed that ANN technique have good potential for predicting the compressive strength and strain at peak stress of concrete, yielding close predictions and good agreement with the original ones.

1. Introduction

In the last nine decades, considerable effort has been spent to understand the inelastic behavior of concrete and the resulting shape of the stress-strain curve. The compressive strength and the strain at peak stress of concrete were found to have a significant interrelationship. Several studies have reported the axial strain capacity to increase significantly in concretes with improved compressive strength. Modern technology and new additives assisted in the improvement of concrete properties. Several parameters influence the strain at peak stress, including water/binder ratio and workability. One measure of quality control and uniformity of concrete from batch to batch is the slump test. Workability extends the fresh use of concrete to achieve full compaction, increase the resistance to bleeding, harshness, and segregation. A significant component that makes up concrete and contributes to its physical improvements is aggregate. A high aggregate/cement ratio indicates lower compressive strength and vice versa.

Some design codes have adopted a constant value for the strain at peak stress of concrete tested under axial compression load. However, such approaches may not yield acceptable results with more minor errors since the compressive strength of concrete and its strain at peak stress are influenced by several parameters such as mixed ingredients, specimen geometry, testing conditions, and environmental conditions.

Several studies have highlighted the potential use of artificial neural networks (ANN) to predict the compressive strength of concrete. In a research, ANN procedure was employed for evaluating the compressive strength of concretes containing metakaolin and silica fume [1] using the experimental test results from 195 specimens produced with 33 different mixture proportions. The obtained test data was used in the multi-layer feed-forward neural network models and were arranged in a format of eight input parameters. In another study, ANNs and genetic programming (GP) were used for predicting the strength of concrete [2]. The ANN model with the training function, Levenberg-Marquardt (LM), was found to be a

Abdulla, N.A. Application of artificial neural networks for prediction of concrete properties. Magazine of Civil Engineering. 2022. 110(2). Article No. 11007. DOI: 10.34910/MCE.110.7

useful tool for compressive strength predictions of concrete. Lai and Serra [3] used the ANN model for assessing the compressive strength of cement conglomerates by constructing models in which a variety of different mix-design parameters associated with cement conglomerates were considered.

Unlike normal concrete, high-strength concrete (HSC) has been reported to be a highly sophisticated material that makes its modeling difficult. ANN models [4] have shown to be a powerful tool for calculating the compressive strength and slump of HSC. The ANN models for compressive strength and slump were constructed, trained, and tested using a database of 187 test results arranged in a format of seven input parameters. The mean absolute percentage error found to be less than 1 % for compressive strength and 5 % for slump values, and the corresponding R^2 values were 99.93 % and 99.34 %, respectively. Naderpour and Mirrashid [5] utilized the ANN technique to assess the effect of micro-silica and calcium in silicate minerals on the compressive strength of mortars. The ANN modeling showed high accuracy, functional ability, and acceptable performance in predicting the compressive strength of the tested mortars. Asteris et al. [6] reported ANN to be a proper simulation technique for predicting concrete properties. Duan et al. [7] suggested an ANN model-based explicit formulation for predicting the loss in compressive strength of recycled aggregate concrete. The authors used one hundred forty-six available sets of data from sixteen different published literature sources to construct ANN models with fourteen input parameters. They concluded that with varying the types and sources of recycled aggregates, ANN showed excellent potential as a technique for evaluating the compressive strength of recycled aggregate concretes.

An experimental program [8] consisting of a direct and indirect evaluation of unconfined compressive strength (UCS) of sixty-six granite and limestone sample sets of rocks was carried out. Point load index test, Schmidt hammer rebound number, p-wave velocity test, and dry density test were used as inputs of the network while the output was the UCS values. A PSO-based ANN techniques hybrid model was proposed. Several studies have reported the predictions of the alternative evaluation methods to be often closer to the experimental test data than the predictions from design codes [9]. ANN method performed better and yielded more accurate predictions than the Multiple Linear Regression (MLR) technique for both slump and compressive strength of concrete [10]. From the above review, most of the previous studies were on the compressive strength of concrete, and the application of the ANN technique to predict the concrete deformation in terms of strain at peak stress still needs to be covered.

The objectives of the present study are to evaluate the previously published models relating the strain at peak stress to the compressive strength; to perform experimental tests to assess the stress-strain relationship parameters, compressive strength and its corresponding compressive strain at maximum stress, of normal strength concrete; to use ANN technique to predict the above two parameters based on the experimental results. Finally, the paper sets to develop a model to predict the strain at peak stress based on regression analysis of ANN predicted values.

2. Materials and Methods

2.1. Materials

The following ingredients were used for the twelve concrete mixtures: water, coarse river aggregate, fine river aggregate, and cement.

Ordinary Portland cement with a specific gravity of 3.15 and conforming to ASTM C150 Type I was used for making concrete.

The coarse aggregate for all the mixes was rounded and well-graded river gravel with a maximum aggregate size of 20 mm and specific gravity of 2.72.

The fine aggregate was river sand from the Eski-kalak region north of Iraq with a maximum size of 4.75mm and specific gravity of 2.7.

The quantity of coarse aggregate was adjusted, yielding twelve mixes with aggregate/cement (a/c) ratios ranging from 3 to 8 in increments of 0.5. Tap water was used to hydrate the ordinary Portland cement in a drum-type rotary mixer. All the mix details are summarized in Table 1.

2.2. Methods of Testing

2.2.1. Fresh concrete

The slump test was used to evaluate the consistency of fresh concrete and the effect of change in the mix on fresh concrete properties. The truncated steel cone was filled with the fresh concrete in three equal layers, and each layer was tamped twenty-five times with a steel rod to ensure compaction. The workability of new concrete decreased as the a/c ratio increased, resulting in harsh combinations with increased compaction difficulties. The details of slump results are presented in Table 1. The unit weight of

fresh concrete was measured and computed in Table 1. In general, as the amount of fine material or sand decreased, the unit weight decreased, too.

2.2.2. Hardened concrete

After 28 days of curing, the rough surface of concrete cylinders was capped with a filling material. The specimens were tested in compression under a displacement control mode at a rate of approximately 0.5 mm/min. The relative displacement between the upper and lower loading platens was measured using two linear variable differential transformer (LVDT) and one dial gauge (Fig. 1). Two electrical strain gauges on the surface of cylinders used for longitudinal and lateral strain measurements. There was an inverse relationship between compressive strength and the three test parameters for hardened concrete depending on variations in constituent materials, Table 1.

2.3. Intelligent systems and methods

2.3.1. Artificial neural networks

The neural network modeling process involves five main aspects: data acquisition, analysis, and problem representation; architecture determination; learning process determination; training of the networks; and testing of the trained system for generalization evaluation [1, 11]. ANN procedure handles severe problems via the interaction between nodes (artificial neurons). The ANN model has elements arranged in layers and trained with the data from the experimental results. The first layers of nodes (neurons) get data from the outside environment and transfer it to the nodes of the hidden layer without performing any computation, where the data is processed to draw out useful features. Weights interconnect other nodes in other layers. The output layer neurons produce network predictions. In a three-layer ANN, training data relates between input and output nodes. Due to the ability of neurons to pass and remember the data from experimental results during the training process, the network can learn, categorize, and predict values.

Table 1. Mix details and properties of fresh and hardened concrete.

Specimen	Mix ratio	w/c ratio	Aggregate/ cement ratio	Slump (mm)	γ (kg/m^3)	f_c (MPa)	ε_c
1-1	1:2:1	0.435	3.0	12	2400	38.7	0.00197
1-2	1:2:1	0.435	3.0	12		38.9	0.0019
1-3	1:2:1	0.435	3.0	12		38.5	0.00192
2-1	1:2:1.5	0.450	3.5	10	2400	36.5	0.00187
2-2	1:2:1.5	0.450	3.5	10		38.1	0.00188
2-3	1:2:1.5	0.450	3.5	10		37.5	0.0018
3-1	1:2:2	0.485	4.0	9.5	2380	34.6	0.00179
3-2	1:2:2	0.485	4.0	9.5		34.3	0.00188
3-3	1:2:2	0.485	4.0	9.5		33.7	0.00182
4-1	1:2:2.5	0.505	4.5	9.5	2375	34	0.00177
4-2	1:2:2.5	0.505	4.5	9.5		32	0.00173
4-3	1:2:2.5	0.505	4.5	9.5		32.7	0.00179
5-1	1:2:3	0.51	5.0	8	2370	31.1	0.00168
5-2	1:2:3	0.51	5.0	8		33.3	0.00176
5-3	1:2:3	0.51	5.0	8		32.2	0.00169
6-1	1:2:3.5	0.51	5.5	7	2355	30.8	0.00172
6-2	1:2:3.5	0.51	5.5	7		32	0.00174
6-3	1:2:3.5	0.51	5.5	7		30.8	0.00171
7-1	1:2:4	0.52	6.0	5	2340	28.5	0.00169
7-2	1:2:4	0.52	6.0	5		29.7	0.00176
7-3	1:2:4	0.52	6.0	5		27.6	0.00169
8-1	1:2:4.5	0.535	6.5	5	2325	25.2	0.00157
8-2	1:2:4.5	0.535	6.5	5		24.8	0.00172
8-3	1:2:4.5	0.535	6.5	5		26.5	0.00182
9-1	1:2:5	0.56	7.0	4	2300	20.6	0.00164

Specimen	Mix ratio	w/c ratio	Aggregate/ cement ratio	Slump (mm)	γ (kg/m^3)	f_c (MPa)	ε_c
9-2	1:2:5	0.56	7.0	4		19.6	0.00165
9-3	1:2:5	0.56	7.0	4		21.6	0.00165
10-1	1:2:5.5	0.585	7.5	2.5	2245	19.9	0.00169
10-2	1:2:5.5	0.585	7.5	2.5		18.2	0.00151
10-3	1:2:5.5	0.585	7.5	2.5		19.5	0.00158
11-1	1:2:6	0.6	8.0	0.0	2270	16.3	0.00153
11-2	1:2:6	0.6	8.0	0.0		16.1	0.00154
11-3	1:2:6	0.6	8.0	0.0		17.7	0.00169
12-1	1:2:6.5	0.605	8.5	0.0	2225	15.6	0.00153
12-2	1:2:6.5	0.605	8.5	0.0		16.85	0.00164
12-3	1:2:6.5	0.605	8.5	0.0		16.4	0.00167

A typical node (AN) designed to carry out specific tasks, as shown schematically in Fig. 2. The network supplied with the values of parameters x_j (selected parameters related to the strength characteristics of the concrete) [9]. Each parameter assigned weight w_{ji} and bias Θ_i and this yields the sum n_i of the multiplication:

$$n_i = \sum\left(x_j\right)\left(w_{ji}\right) + \theta_i \tag{1}$$

The n_i is integrated into an established activation function (g):

Figure 1. Testing of concrete specimens.

$$y_i = g_i = g\left(\sum\left(x_i\right)\left(w_{ji}\right) + \theta_i\right) \tag{2}$$

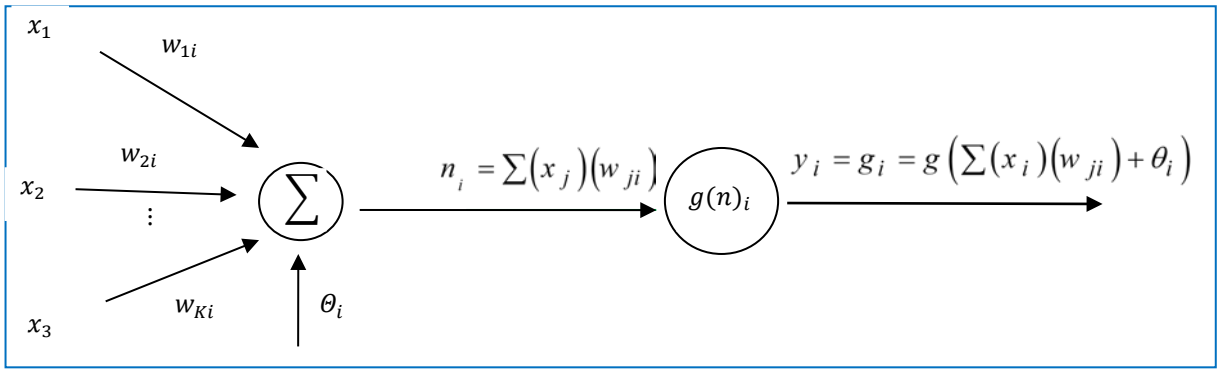

Figure 2. A simple neuron model.

And the result is the output O_i of the AN. Several layers assembled to establish the artificial neural networks used in the present study. The randomly assigned values of the weights and bias undergo iterative training to yield the final results. The architecture of the ANN established through a trial-and-error process related to the type of activation function and the number of neurons in each hidden layer. The goal of this process is to reduce the gap between the ANN output O_i values and the target values T_i [12, 13, 1]. A measure of the deviation of O_i from T_i is given by:

$$E = \frac{1}{2}\sum(T_i - O_i)^2 \quad (3)$$

2.3.2. Adopted ANN models

The three-layer feed-forward type of ANNs was adopted in the present study, Figs. 3 to evaluate the peak stress and Fig.4 to assess the strain at peak stress. The transferred information is processed to extract useful features to reconstruct the architecture from the input space to the output space [15]. If convergence is not achieved, the calculation repeated. Weights fully interconnect the neighboring layers. The network architecture is dictated by the interconnected input, hidden, and output neurons. The weights and processing function of each neuron influence the output layer.

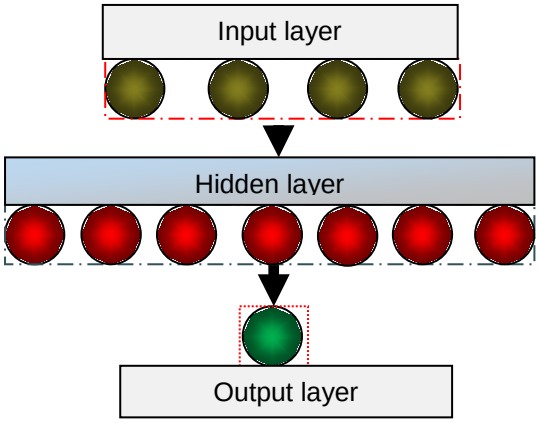

Figure 3. Architecture of ANN model to evaluate peak stress.

Most studies adopted a neural network with one hidden layer that was found sufficient to solve most problems in civil engineering [16–18]. When considering computational efforts required for more hidden layers and an additional number of neurons, one hidden layer reported to be sufficient to produce an acceptable ANN model [19] and to predict the elastic modulus of concrete. When increasing the number of hidden layers, a marginal change in results was obtained [20]. Two ANN models, ANN-1 and ANN-2, with one hidden layer were constructed, trained, and tested using the current experimental test results. The experimental test data was based on two different mix parameters (i.e., w/c and a/c ratios) in addition to slump results. The experimental data was divided into three subcategories of training, validation, and test. Subsequently, the network was trained to minimize the error between the experimental and ANN predicted values.

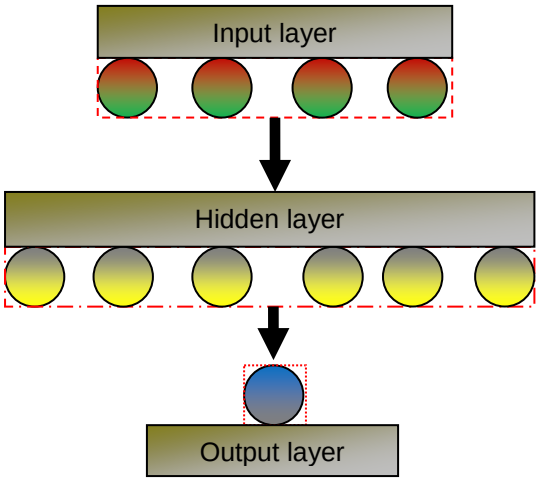

Figure 4. Architecture of ANN model to evaluate strain at peak stress.

The two concrete mix parameters (w/c ratio and a/c ratio) and slump values were used as the four input variables and the bias. The compressive strength and strain at peak stress were the output parameters for the two models, as shown in Figs. 3 and 4, respectively. The hidden layer of the ANN-1 Model to evaluate peak stress (Fig. 3) consisted of seven neurons. In contrast, the same number for the ANN-2 Model to evaluate strain consisted of six neurons (Fig. 4).

3. Results and Discussions

3.1. Strain models

The size and shape of the specimen and concrete physical characteristics influence the strain at peak stress of concrete [21]. Strain is needed to determine the response of a structure to crack control and assess cracking risk [22]. Generally concrete strain is expressed as a function of compressive strength in standard codes and empirical expressions. Different function forms of $\varepsilon_c - f_c$ relationship is found in the literature which can be classified into three groups. The experimental test results were checked against the three groups containing fifty-three existing expressions for strain at peak stress [21–68]. It included the following:

3.3.1. Group one (G-1) with polynomial function

In models with polynomial functions [21, 22, 27], the compressive strength is raised to a non-negative integer power. The leading term or the highest power of the variable in the polynomial function was 3. Among the three models in group one is the model by Tasdemir et al. [22], which was based on tests on concrete with a wide range of strengths from 6 to 105 N/mm^2. Using a total of 228 test results for specimens tested under uniaxial compressive loading conditions, the authors reported a polynomial function to best fit the experimental data with a reasonably good correlation coefficient of 0.75, Table 2.

3.3.2. Group two (G-2) with linear function

Twenty-one models [24–26, 28, 30, 32, 33, 35, 36, 38–40, 47, 49, 54, 56, 59, 60, 62, 63, 65] among the fifty-three models have a linear function. Group two linear models with large database include two models; Chen et al. [60] and Chen et al. [63] with 380 test data from 15 studies.

3.3.3. Group three (G-3) with power functions

The largest group with twenty-nine models [23, 29, 32, 34, 37, 39, 41–46, 48, 50–53, 55, 57, 58, 61, 64, 66a, 67, 68]. Several of these models based on a large database, including De Nicolo et al. [39] using 17 studies, Arıoğlu [42] with 41 sets of test data from 8 studies, Wee et al.[44] with 163 test data, Mansur et al. [48] with 54 test data, Lu and Zhao [55] with 75 test data, Ding et al. [57] with 165 test data, Kumar et al. [58] with 162 test results, Lim and Ozbakkaloglu [61] with 147 test data, Hoang and Fehling [67] with 132 test data from 6 studies. All the equations with a power function have a variable base as a compressive strength raised to power with a small, even positive number. The power ranges from 0.19 [66] (a) to 0.53 [52] and [66]c for most of the studies. However, the model [67] uses power as high as 0.96. On the other hand, the model [68] incorporates negative power (-2.256).

Other studies, not included in Table 2, employed constant values of strain such as 0.002 [44, 69], 0.0022 [70–73], 0.0024 [74], and 0.003 [75, 76]. The ε_c =0.003 was suggested to be used for design purposes, for concrete compressive strengths up to 124MPa [75, 76].

Table 2. Models used to predict the strain at peak stresses.

Year	Source	Model	Strength range MPa	No. of test data	Comments
1993	Collins et al. [21]	$\varepsilon_c = \frac{f_c\left(0.0588 f_c + 0.8\right)}{\left(3220 {f_c}^{0.5} + 6900\right)\left(0.0588 f_c - 0.2\right)}$ ε_c is strain at peak stress f_c is compressive strength	21 to 83MPa	14	
1998	Tasdemir et al.[22]	$\varepsilon_c = \left(-0.067 \frac{{f_c}^2}{{f_c}^*} + 29.9 \frac{f_c}{{f_c}^*} + 1053\right) 10^{-6}$ f^* = 1 MPa	6 to 105MPa	228 from 12 studies	R^2= 0.75

Year	Source	Model	Strength range MPa	No. of test data	Comments
1936	Emperger [23]	$\varepsilon_c = \left(0.0445\left(f_c\right)^{0.5}\right)10^{-2}$			For concrete with a low level of sand
1950	Ros [24]	$\varepsilon_c = \left(0.0546 + 0.003713 f_c\right)10^{-2}$			
1955	Hognestad et al. [25]	$\varepsilon_c = \left(0.004 + \frac{f_c}{6.5_c}\ 10^{-6}\right)$	5 to 52.4	26	
1962	Liebenberg [26]	$\varepsilon_c = \left(0.004 + \frac{f_c}{(0.73)(8.3)}10^{-6}\right)$	7 to 69		
1964	Saenz [27]	$\varepsilon_c = 0.12\left(f_c\right)^{0.25}\left[9 - \left(f_c\right)^{0.25}\right]10^{-3}$			
1967	Soliman et al.[28]	$\varepsilon_c = 2\left(f_c\right)/25097^{*}$ *MPa		16	
1970	Popovics [29]	$\varepsilon_c = 0.000735\left(f_c\right)^{0.25}$			
1970	Tadros [30]	$\varepsilon_c = \left(1.6 + 0.01 f_c\right)10^{-3}$			
1973	Popovics [31]	$\varepsilon_c = 0.000937\left(f_c\right)^{0.25}$			Curve fitting using data from another reference
1976	Bashur and Darwin[32]	$\varepsilon_c = \frac{f_c}{363000 + 400 f_c}$ (f_c in psi)	(f_c in psi)		Curve fitting using data from another
1982	Ahmad-Shah [33]	$\varepsilon_c = 0.001648 + 1.65\left(f_c\right)10^{-5}$	20 to 75		
1984	Tomaszewicz [34]	$\varepsilon_c = 700\left(f_c\right)^{0.31}10^{-6}$	f_c≤ 85MPa		High-strength
1985	Shah-Fafitis [35]	$\varepsilon_c = 1.491\left(10^{-5}\right)\left(f_c\right) + 0.00195$			
1986	Carreira-Chu [36]	$\varepsilon_c = 0.71\left(10^{-5}\right)\left(f_c\right) + 0.00168$	8.96 to 52.4	9	Data from two studies
1990	Ali et al. [37]	$\varepsilon_c = 0.000875\left(f_c\right)^{0.25}$	16.7 to 43.5	12	
1994	Hsu and Hsu [38]	$\varepsilon_c = 1.29\left(10^{-5}\right)\left(f_c\right) + 2.114\left(10^{-3}\right)$	65.8 to 91.4	14	
1994	De Nicolo et al. [39]	$\varepsilon_c = 0.00076 + \left[\left(0.626\frac{f_c}{f^{*}} - 4.33\right)10^{-7}\right]^{0.5}$	10 MPa≤ f_c≤ 100 MPa	Not given 17 studies	
	Brandtzaeg [39]	$_c = \frac{f_c}{46.886 + 2.6 f_c}10^{-2}$			
1995	Almusallam and Alsayed [40]	$\varepsilon_c = \left(0.398 f_c + 18.147\right)10^{-4}$	20 to 110MPa		
1995	CEB-FIB [41]	$\varepsilon_c = \left(0.7 f_c\right)^{0.31}\left(10^{-3}\right)$	fc≤ 100MPa		
1995	Arıoğlu [42]	$\varepsilon_c = 1.753\left(f_c\right)^{0.27756}\left(V\right)^{-0.09314}$	V=volume	41 from 8 studies	R^2= 0.874

Year	Source	Model	Strength range MPa	No. of test data	Comments
1996	Attard and Setunge [43]	$\varepsilon_c = \frac{3.78 f_c}{E_c \sqrt[4]{f_c}}$	> 40MPa		
1996	Wee et al.[44]	$\varepsilon_c = 0.00078 (f_c)^{0.25}$		163	
1997	Guo [45]	$\varepsilon_c = \left(700 + 172\left(\sqrt[2]{f_c}\right)\right)10^{-3}$	Up to 120MPa		
1998	Xu [46]	$\varepsilon_c = \left(966 + 155.64\left(\sqrt[2]{f_c - 13.77}\right)\right)10^{-3}$			high-performance concrete
1999	CEB-FIB [47]	$\varepsilon_c = \left(1.7 + \frac{f_c}{f_{cmo}}\right)10^{-3}$	f_{cmo}=70, f_c≤100MPa f_c≤100MPa		
1999	Mansur et al. [48] a	$\varepsilon_c = 0.0005 (f_c)^{0.35}$	70 to 120MPa	54	For cylinders
1999	Mansur et al. [48] b	$\varepsilon_c = 0.00048 (f_c)^{0.35}$	70 to 120MPa	54	For prisms
2002	Lee [49] c	$\varepsilon_c = \frac{f_c}{(46.886 + 2.6 f_c)10^2}$	75 to 78	20 HPC	
2003	NS 3473[50]	$\varepsilon_c = \frac{0.7}{1000}(f_c)^{0.31}$	f_c=peak stress		
2003	Yu and Ding [51]	$\varepsilon_c = \left(383 f_{cu}^{7/18}\right)10^{-6}$			$f_c = 0.4 f_{cu}^{7/6}$
2004	EC2 [52]	$\varepsilon_c = 2 + 0.085 (f_c - 50)^{0.53}$	50MPa≤f_c≤ 100MPa		0.002 for f_c<50MPa
2004	Tasnimi [53]	$\varepsilon_c = \left(65.57 f_c^{0.44} - 6.748\right)10^{-5}$			
2006	Mertol [54]	$\varepsilon_c = 0.0033 - 13.793\left(10^{-5}\right) f_c$	69 to 124	21	
2008	Lu and Zhao [55]	$\varepsilon_c = 430 (f_c)^{0.38}\left(10^{-6}\right)$	42.7 to 125.6	75	
2010	Arslan and Cihanli[56]	$\varepsilon_c = 0.002 + \left(\frac{0.001(f_c - 20)}{70}\right)$	50MPa≤f_c< 100MPa		
2011	Ding et al. [57] a	$\varepsilon_c = 520 (f_c)^{1/3}\left(10^{-3}\right)$	20 to 150MPa from five studies	165groups	
2011	Ding et al. [57] b	$\varepsilon_c = 383 (f_{cu})^{7/18}\left(10^{-6}\right)$	30 to 150MPa from four	58 groups	$f_c = 0.4 f_{cu}^{7/6}$
2011	Kumar et al. [58]	$\varepsilon_c = 0.0006 (f_c)^{1/3}\left(10^{-3}\right)$	35 to 70MPa	162 cylinders	self-compacting concrete
2013	Hussin et al. [59]	$\varepsilon_c = 2 (f_c)\left(10^{-5}\right) + 0.0008$	9.25 to 38	26	
2013	Chen et al.[60]	$\varepsilon_c = 1.74 (f_c)\left(10^{-6}\right) + (2.41)\left(10^{-3}\right)$	HSC considering size effect	380 from 15 studies	COV=0.176

Year	Source	Model	Strength range MPa	No. of test data	Comments
2014	Lim and Ozbakkaloglu[61]	$\varepsilon_c = \left(f_{co}^{\,0.225k_d}\right)\left(10^{-3}\right)k_s k_a$ $k_s = 1, k_a = 1$	10MPa≤f_c≤ 150MPa	147	R^2=0.626 NWC
2015	Ahmed et al.[62]	$\varepsilon_c = 0.00003\left(f_c\right) + 0.001$	5.9 to 26.5	78	R^2=0.49
2015	Chen et al.[63]	$\varepsilon_c = 4.76\left(f_c\right)10^{-6} + \left(2.13\right)10^{-3}$	20 to 105	380 from 15 studies	COV=0.14
2016	Wang et al. [64]	$\varepsilon_c = 0.5\left(1.95 + 0.01491 f_c + 0.763\sqrt[4]{f_c}\right)$	f_c≤200MPa		
2016	Shanaka [65]	$\varepsilon_c = 1.1\left(\frac{f_c}{E_c}\right)$	95 to 147MPa	18	
2016	Nematzadeh et al.[66] a	$\varepsilon_c = \left(1074 f_c^{\,0.19}\right)10^{-6}$	17.9-52.6MPa RC	30	R^2=0.62, reference concrete (RC)
2016	Nematzadeh et al.[66] b	$\varepsilon_c = 402\left(10^{-6}\right)\left(f_c^{\,0.41}\right)$	43-83MPa LPCC	30	R^2=0.55, long-term pressure-compressed concrete
2016	Nematzadeh et al.[66] c	$\varepsilon_c = 225\left(10^{-6}\right)\left(f_c^{\,0.53}\right)$	44-91MPa SPCC	30	R^2=0.74,Short-term pressure-compressed concrete
2017	Hoang and Fehling[67]	$\varepsilon_c = 0.0257\left(10^{-2}\right)\left(f_c^{\,0.96}\right)$	100≤f_c ≤150MPa	132 from 6 studies	R^2=0.86, UHPC; Ultra-high performance concrete
2017	Aslam et al.[68]	$\varepsilon_c = 18.938\left(f_c\right)^{-2.256}$	42.5 to 52	9 *LWA*	R^2=0.96
	Proposed	$\varepsilon_c = 0.001\left(f_c\right)^{0.17}$	16.1 to 38.9MPa	36	R^2=0.82

3.2. ANN models

A total of 36 data sets with minimum and maximum concrete strengths of 15.6 MPa and 38.9MPa were unequally divided and used for training (approximately 80% of modeling) and the rest for testing (about 20%) of the model. The ANN approach considers several parameters affecting the strength of

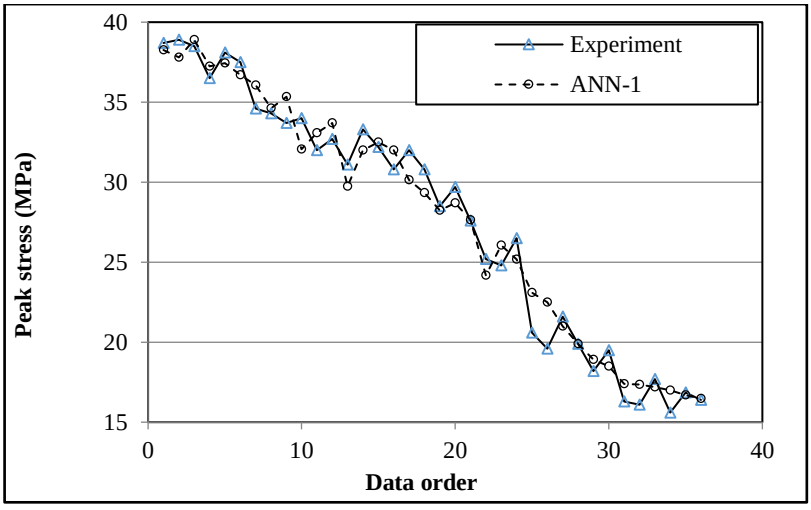

Figure 5. Comparison of predicted peak stress (ANN-1) with experimental peak stress.

concrete at the same time [19]. The experimental compressive strength and predicted strength values using the ANN-1 model were plotted in Fig.5. A similar procedure followed for strain at peak stress, using ANN-2 model, as shown in Fig. 6. The results showed that, on average, the peak stress decreased as aggregate/cement ratio and w/c ratio increased.

In Figure 6, the trend for the experimental strain was more to increase with a decrease in the aggregate/cement ratio, and this follows the same trend for predicted strain at peak stress using the ANN-2 model. ANN models have captured the inter-relationships between input and output data pairs. The curves plotted in Fig. 5 for peak stress and Fig. 6 for corresponding strain demonstrate that the neural network was effective in learning the relationship between the different input parameters and the outputs, compressive strength, and strain at peak stress. The error between the predicted and experimental values then was computed. The output error can be minimized by modifications on the weights and bias at each neuron. The connections which could be positive or negative were not shown in Figs. 3 and 4. Instead, all the connection weights and biases used to predict the peak stress of concrete were computed in Table 3, and the connection weights and biases used to predict the strain at peak stress of concrete were summarized in Table 4.

Table 3. Connection weights and biases used to predict the strength of concrete.

Neuron	w/c	a/c	Slump	(Bias)
1	-0.423	0.242	0.205	-0.152
2	.171	.039	-.208	.338
3	-.284	-.205	.190	.380
4	-.868	-.319	-.083	.046
5	.347	.293	-.109	.230
6	.437	.404	.066	.075

Neuron	1	2	3	4	5	6	(Bias)
fco	0.144	-0.177	0.326	0.673	0.027	-0.481	-0.010

Table 4. Connection weights and biases used to predict the peak strain of concrete.

Neuron	w/c	a/c	slump	(Bias)
1	-.346	-.246	.509	-.732
2	-.729	.447	.136	-.078
3	.703	-.697	.174	-.034
4	.568	-.286	.072	.132
5	.053	-.340	-.915	.951

Neuron	1	2	3	4	5	(Bias)
Strain	0.538	0.709	-0.820	-0.441	-1.176	1.013

In normal strength concretes the elastic mismatch of aggregate and the matrix is significant, leading to large tangential, radial, and shear stresses at the paste-aggregate interface [22]. In the current study, the predicted peak strain values, using ANN-2 model, were plotted versus the corresponding predicted maximum stress, using the ANN-1 model and the graph was fitted with a nonlinear curve to find the relationship between the two variables. Consequently, an equation obtained and proposed for peak strain predictions, as summarized in Table 2.

3.3. Statistical indices

Several standard statistics used to assess the performances of the existing fifty-three equations for the strain at peak stress which include:

3.3.1. Normalized root-mean-square error (NRMSE)

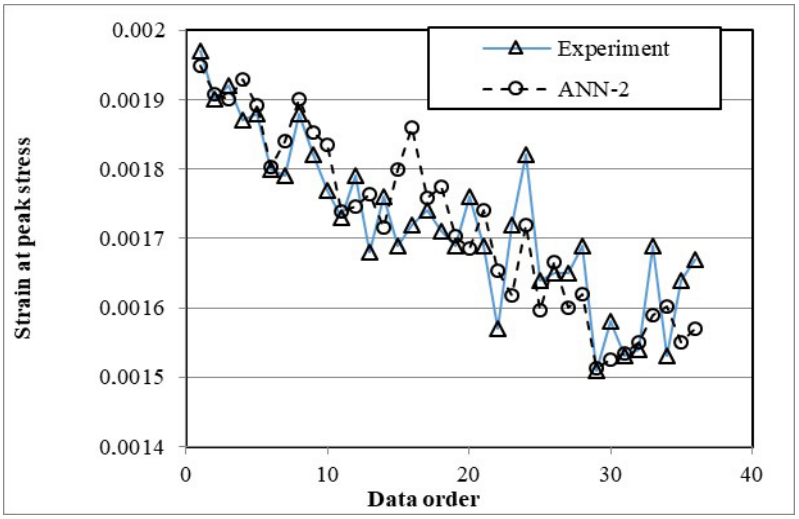

Figure. 6. Comparison of predicted strain at peak stress (ANN-2) with the corresponding experimental values.

$$NRMSE = \frac{\sqrt{\sum_{i=1}^{N}\left(\exp._i - model_i\right)^2}}{\sum_{i=1}^{N}\exp._i} \quad (4)$$

Where the model prediction is expressed by ($model._i$), the experimental value is represented by ($exp.i$), and N is the total number of data.

3.3.2. Average absolute error (AAE)

$$AAE = \frac{\sum_{i=1}^{N}\left|\frac{model_i - \exp._i}{\exp._i}\right|}{N} \quad (5)$$

Lower AAE values indicate excellent model performance.

3.3.3. Nash–Sutcliffe efficiency (E)

$$E = 1 - \frac{\sum_{i=1}^{N}\left(\exp._i - model_i\right)^2}{\sum_{i=1}^{N}\left(\exp._i - aver.\exp._i\right)^2} \quad (6)$$

An E value of over 0.80 is considered good.

3.3.4. Modified Nash–Sutcliffe efficiency (E1)

$$E1 = 1 - \frac{\sum\left|\exp._i - model_i\right|}{\sum\left|\exp._i - aver.\exp._i\right|} \quad (7)$$

The Modified Nash–Sutcliffe efficiency is based on absolute deviations instead of squares of the deviations.

3.3.5. Coefficient of correlation (R^2)

$$R^2 = \left(\frac{\sum_{i=1}^{N}\left(\exp._i - aver.\exp._i\right)\left(model_i - model_i aver\right)}{\sum_{i=1}^{N}\left(\exp._i - aver.\exp._i\right)^2 \sum_{i=1}^{N}\left(model_i - model_i aver\right)^2}\right)^2 \quad (8)$$

R^2 is the rate of association between the two variables, and many outliers result in weak R^2. The statistical measures also used to determine the performance of the two trained ANN models.

3.4. Strain at peak stress

The fifty-three existing strain models found in the literature [21-68] and the proposed ANN-based model were used to predict the strains (ε_c) at the peak stress and were compared with the experimental results. All the models for the strain at peak stress prediction summarized in Table 2 including the proposed ANN-based model. Some models have limitations that make these models not applicable to the strength range of the present study, but were included for comparison purposes. The predicted strains and the best fitting line or curve for each model shown in Fig. 7 for G-1 models with polynomial functions. Also shown in Fig.7 is the predictions by the proposed ANN-based model. A significant trend is observed as the compressive stress of concrete increases, the strain at peak stress increases, too [21, 22, 27]. The same thing is correct for the proposed equation. Model [22] exhibit good predictions for concrete strengths up to 25MPa. However, at strengths beyond 25Mpa the error increases. The model [27] show a reasonable performance for all the strength range tested in the present study. The third model in G-1 over predicts the strain values, Fig.7. The proposed strain equation out performed all the three models in G-1 with very good predictions, Fig.7.

Fig. 8 shows predictions and best-fitting lines for the models with linear function in addition to the proposed model. The predicted strains spread over a wide strain range, 0.0001 to 0.004. The best-fitting lines or curves for some of the models [28, 40,49, 54] become steeper away from the origin. All models prediction show an increase in compressive strength, except the EC2 model, which shows a reverse trend because it is proposed for strengths higher than 50 MPa, which is beyond the experimental strength range covered in the present study. As can be seen, most of the models overestimated the strain values, and some models largely over-predicted the experimental strain values [25, 26, 40]. Using model [24], a better prediction of strain at lower values of f_c is observed. The opposite can be said for other models [28].

The predictions of models using power functions are displayed in Fig. 9. The predictions with best-fitting curves in Fig. 9 compared with Fig. 8 are more compact with fewer models overestimating the predicted strain values, except for model 67 which was proposed for ultra-high-strength concrete. In contrast to models with a linear function, only a couple of models with power functions underestimated the values for the strain at peak stress, [57]a and [66]c. Some models showed a better prediction of strain at lower values of f_c, example model [23]. This trend is reversed in the predictions of other models, such as model [55]. Over all, the models with linear functions, Fig. 8, displayed more change in the best-fitting line slope than models in Fig.9. Most existing model predictions are higher than the test data and the proposed model, this is ascribed to the fact that these models were developed for concretes with higher strength.

3.5. $\varepsilon_{c\,Pre}/\varepsilon_{c\,Exp}$ ratio

To further assess the performance of the fifty-three existing models and the proposed model, the ratio of the predicted strain ($\varepsilon_{c\,Pre}$) to the experimental strain ($\varepsilon_{c\,Exp}$) at peak stress was computed and shown in Table 5. Five statistical indexes used to evaluate the percentage of error or the degree of association between the experimental test results and their corresponding predicted values. The difference between the experimental and predicted values of the strain at peak stress was summarized in Table 6. Other statistical indexes including minimum predictions (Min.), maximum predictions (Max.), mean, standard deviation (STD), and coefficient of variance (COV) are also shown in Table 6. Lower values of NRMSE and AAE show good performance of the models. In contrast, higher values of E, $E1$, and R^2 show less error measured between the predicted and experimental values.

Statistics on the performance of fifty-three existing models and the proposed model illustrate that the values of NRMSE ranged from 0.0011(proposed model) to 0.27 [68] and for AAE ranged from 3.46% (proposed model) to 785.81% [68]. A similar observation made for the other indexes. The six models with least values of NRMSE and AAE included the proposed model, [44], [51], [58], [33], and [27] with values of 0.0011, 0.0014, 0.0019, 0.0018, 0.0021, 0.0025 and 3.46%, 4.445% , 5.34%, 5.712%, 6.072%, 6.761% respectively. Among the six models with the least values of NRMSE and AAE, four models have power function, one model with a linear function, and one model with a polynomial function. This indicates that models with power functions showed better performance compared with the other two types of models. Ahmed-Shah's [33] model with a linear function yielded nearly a horizontal best-fitting line and shows reasonable predictions with NRMSE and AAE values of 0.0025 and 6.761%, respectively. For the range of strength considered in the present study, the constant value of the model [33] controls the outcome of the strain values with the variable parameter (f_c) having a minor role. The model [44] with AAE values of 4.445% displayed reasonable predictions of strain. The proposed model with AAE values of 3.46% yielded the lowest AAE values with predictions of strain at peak stress very close to the experimental strain values. The proposed model showed good performance with the highest values of E and E1. Furthermore, the

proposed model yielded the lowest values of NRMSE among all the models, as shown in Fig. 10. The R^2 value for the proposed model (0.708) was slightly lower than for models [35, 36] with similar values of 0.736, Table 6. Few equations found to reasonably predict the strains at peak stress for the different concrete mixtures. As it was explained before, several existing strain models have been calibrated for high-strength concrete and show poor performance when used to predict the strain of normal strength concrete. Furthermore, most of these models derived from simple regression analysis based on test results carried out by the generators of the models and applicable for a particular type of concrete. Several of these expressions are valid within limited ranges of strength and not for other varieties. The complex relations developed between the mix proportions of concrete and the compressive strength can be captured better by the ANN-based model, which trained to yield low mean squared error and absolute average error between the experimental results and the network predicted values.

Table 5. The ratio of $\varepsilon_{c\ Pre}/\varepsilon_{c\ Exp}$ using existing fifty-three models and the proposed model.

	$\varepsilon_{c\ Pre}/\varepsilon_{c\ Exp}$														
Specimen	[21]	[22]	[23]	[24]	[25]	[26]	[27]	[28]	[29]	[30]	[31]	[32]	[33]	[34]	[35]
1-1	1.081	1.071	1.405	1.007	2.033	2.034	0.988	1.565	0.931	1.009	1.186	1.092	1.161	1.104	1.283
1-2	1.122	1.113	1.461	1.048	2.108	2.108	1.026	1.632	0.966	1.047	1.232	1.133	1.205	1.146	1.332
1-3	1.107	1.096	1.438	1.029	2.086	2.086	1.013	1.598	0.954	1.034	1.216	1.12	1.189	1.131	1.315
2-1	1.121	1.099	1.438	1.017	2.142	2.142	1.032	1.555	0.966	1.051	1.232	1.141	1.203	1.142	1.334
2-2	1.128	1.114	1.461	1.043	2.131	2.131	1.033	1.615	0.971	1.054	1.238	1.142	1.211	1.151	1.339
2-3	1.173	1.156	1.514	1.077	2.225	2.225	1.077	1.66	1.01	1.097	1.288	1.19	1.259	1.196	1.394
3-1	1.156	1.121	1.462	1.023	2.238	2.238	1.069	1.54	0.996	1.087	1.27	1.183	1.24	1.173	1.378
3-2	1.098	1.064	1.386	0.968	2.13	2.13	1.016	1.454	0.946	1.034	1.206	1.125	1.178	1.114	1.309
3-3	1.13	1.09	1.419	0.988	2.201	2.201	1.047	1.476	0.973	1.064	1.24	1.158	1.211	1.144	1.348
4-1	1.164	1.126	1.466	1.022	2.263	2.263	1.078	1.531	1.003	1.096	1.278	1.193	1.248	1.18	1.388
4-2	1.174	1.122	1.455	1.002	2.315	2.315	1.092	1.474	1.01	1.11	1.288	1.209	1.258	1.185	1.403
4-3	1.141	1.094	1.422	0.983	2.237	2.237	1.059	1.456	0.982	1.077	1.252	1.172	1.222	1.153	1.362
5-1	1.202	1.142	1.477	1.012	2.384	2.384	1.12	1.475	1.033	1.138	1.317	1.239	1.286	1.209	1.437
5-2	1.165	1.122	1.459	1.013	2.276	2.276	1.081	1.508	1.003	1.098	1.279	1.196	1.249	1.179	1.39
5-3	1.204	1.152	1.494	1.031	2.37	2.37	1.119	1.518	1.036	1.137	1.321	1.239	1.29	1.215	1.438
6-1	1.172	1.111	1.436	0.982	2.328	2.328	1.092	1.427	1.007	1.109	1.283	1.208	1.254	1.178	1.401
6-2	1.168	1.116	1.447	0.997	2.302	2.302	1.086	1.466	1.005	1.103	1.281	1.202	1.251	1.178	1.395
6-3	1.179	1.117	1.444	0.988	2.342	2.342	1.098	1.435	1.013	1.116	1.291	1.215	1.261	1.185	1.409
7-1	1.174	1.095	1.406	0.949	2.369	2.369	1.097	1.344	1.005	1.115	1.281	1.213	1.253	1.17	1.405
7-2	1.137	1.069	1.378	0.937	2.275	2.275	1.061	1.345	0.975	1.078	1.243	1.173	1.215	1.138	1.36
7-3	1.168	1.081	1.383	0.929	2.369	2.369	1.092	1.301	0.997	1.11	1.271	1.206	1.245	1.158	1.397
8-1	1.239	1.124	1.423	0.944	2.55	2.55	1.158	1.279	1.049	1.18	1.337	1.276	1.315	1.212	1.481
8-2	1.128	1.019	1.288	0.853	2.328	2.328	1.054	1.149	0.954	1.074	1.216	1.161	1.196	1.101	1.349
8-3	1.077	0.988	1.259	0.841	2.2	2.2	1.007	1.16	0.916	1.025	1.168	1.111	1.146	1.062	1.289
9-1	1.161	1	1.232	0.799	2.441	2.441	1.071	1.001	0.955	1.101	1.217	1.169	1.212	1.09	1.376
9-2	1.151	0.978	1.194	0.772	2.426	2.426	1.055	0.947	0.937	1.088	1.195	1.148	1.195	1.067	1.359
9-3	1.158	1.011	1.253	0.817	2.426	2.426	1.073	1.043	0.96	1.101	1.224	1.175	1.215	1.1	1.377
10-1	1.125	0.959	1.175	0.76	2.369	2.369	1.033	0.938	0.919	1.064	1.171	1.125	1.169	1.047	1.329
10-2	1.255	1.043	1.257	0.809	2.651	2.651	1.138	0.961	1.005	1.18	1.282	1.232	1.29	1.14	1.471
10-3	1.202	1.019	1.244	0.804	2.534	2.534	1.101	0.984	0.978	1.136	1.246	1.198	1.247	1.113	1.418
11-1	1.241	0.995	1.174	0.752	2.616	2.616	1.102	0.849	0.965	1.152	1.231	1.181	1.253	1.087	1.433

	$\varepsilon_{c\,Pre}/\varepsilon_{c\,Exp}$														
Specimen	[21]	[22]	[23]	[24]	[25]	[26]	[27]	[28]	[29]	[30]	[31]	[32]	[33]	[34]	[35]
11-2	1.234	0.985	1.159	0.743	2.599	2.599	1.092	0.833	0.956	1.144	1.219	1.169	1.243	1.076	1.422
11-3	1.121	0.924	1.108	0.712	2.368	2.368	1.012	0.835	0.892	1.051	1.137	1.093	1.148	1.009	1.31
12-1	1.244	0.982	1.149	0.735	2.616	2.616	1.093	0.813	0.955	1.148	1.217	1.166	1.245	1.072	1.427
12-2	1.157	0.938	1.114	0.714	2.441	2.441	1.034	0.819	0.908	1.078	1.158	1.112	1.174	1.024	1.342
12-3	1.137	0.913	1.079	0.692	2.397	2.397	1.01	0.783	0.886	1.056	1.129	1.084	1.149	0.998	1.314

Table 5 continued.

	$\varepsilon_{c\,Pre}/\varepsilon_{c\,Exp}$														
Specimen	[36]	[37]	[38]	[39]	[39]b	[40]	[41]	[42]	[43]	[44]	[45]	[46]	[47]	[48]a	[48]b
1-1	0.992	1.108	1.327	1.102	1.332	1.703	1.104	1.237	1.218	0.988	0.898	0.885	1.144	0.912	0.876
1-2	1.03	1.15	1.377	1.145	1.383	1.77	1.146	1.284	1.265	1.025	0.933	0.919	1.187	0.948	0.91
1-3	1.017	1.135	1.36	1.128	1.364	1.743	1.131	1.267	1.247	1.012	0.92	0.906	1.172	0.935	0.897
2-1	1.037	1.15	1.382	1.134	1.377	1.747	1.142	1.282	1.255	1.025	0.93	0.913	1.188	0.942	0.904
2-2	1.038	1.156	1.386	1.147	1.389	1.772	1.151	1.29	1.269	1.031	0.937	0.922	1.194	0.951	0.913
2-3	1.081	1.203	1.443	1.191	1.443	1.837	1.196	1.342	1.317	1.072	0.974	0.958	1.242	0.988	0.948
3-1	1.076	1.186	1.43	1.16	1.413	1.783	1.173	1.32	1.285	1.057	0.956	0.937	1.226	0.966	0.927
3-2	1.023	1.126	1.36	1.101	1.341	1.691	1.114	1.253	1.219	1.004	0.908	0.889	1.165	0.917	0.88
3-3	1.055	1.158	1.4	1.129	1.377	1.734	1.144	1.288	1.251	1.033	0.933	0.913	1.199	0.941	0.903
4-1	1.086	1.194	1.442	1.165	1.42	1.79	1.18	1.328	1.291	1.064	0.962	0.941	1.235	0.971	0.932
4-2	1.102	1.203	1.461	1.164	1.422	1.785	1.185	1.336	1.29	1.072	0.967	0.943	1.247	0.972	0.933
4-3	1.068	1.169	1.417	1.134	1.385	1.741	1.153	1.299	1.257	1.042	0.941	0.918	1.211	0.947	0.909
5-1	1.131	1.23	1.497	1.185	1.449	1.817	1.209	1.365	1.314	1.096	0.988	0.961	1.276	0.991	0.951
5-2	1.089	1.194	1.445	1.162	1.418	1.784	1.179	1.328	1.288	1.065	0.962	0.94	1.236	0.969	0.93
5-3	1.129	1.233	1.497	1.194	1.459	1.832	1.215	1.37	1.324	1.099	0.992	0.967	1.278	0.997	0.957
6-1	1.104	1.198	1.46	1.153	1.41	1.768	1.178	1.33	1.279	1.068	0.962	0.935	1.244	0.965	0.926
6-2	1.096	1.196	1.452	1.157	1.414	1.775	1.178	1.328	1.283	1.066	0.961	0.937	1.24	0.967	0.928
6-3	1.11	1.205	1.469	1.159	1.419	1.778	1.185	1.337	1.286	1.075	0.968	0.941	1.251	0.97	0.932
7-1	1.114	1.196	1.468	1.137	1.394	1.745	1.17	1.324	1.263	1.066	0.958	0.925	1.247	0.956	0.917
7-2	1.074	1.161	1.419	1.11	1.36	1.703	1.138	1.286	1.232	1.035	0.93	0.902	1.207	0.931	0.894
7-3	1.11	1.187	1.462	1.123	1.376	1.724	1.158	1.313	1.247	1.058	0.949	0.914	1.239	0.945	0.907
8-1	1.184	1.249	1.554	1.165	1.428	1.795	1.212	1.378	1.295	1.113	0.996	0.95	1.312	0.985	0.946
8-2	1.079	1.135	1.415	1.057	1.295	1.629	1.101	1.252	1.175	1.012	0.905	0.862	1.194	0.894	0.859

8-3	1.026	1.091	1.349	1.026	1.258	1.577	1.062	1.205	1.14	0.972	0.871	0.836	1.142	0.865	0.83
9-1	1.114	1.137	1.451	1.028	1.251	1.606	1.09	1.247	1.143	1.013	0.903	0.837	1.216	0.879	0.844
9-2	1.103	1.116	1.434	1.001	1.214	1.573	1.067	1.223	1.114	0.995	0.886	0.813	1.2	0.859	0.824
9-3	1.111	1.143	1.45	1.042	1.27	1.621	1.1	1.256	1.158	1.019	0.909	0.849	1.217	0.888	0.853
10-1	1.078	1.094	1.403	0.983	1.194	1.542	1.047	1.199	1.094	0.975	0.868	0.8	1.174	0.843	0.809
10-2	1.198	1.197	1.555	1.06	1.279	1.681	1.14	1.309	1.18	1.067	0.95	0.857	1.298	0.914	0.878
10-3	1.151	1.164	1.497	1.043	1.265	1.64	1.113	1.275	1.16	1.037	0.924	0.847	1.252	0.895	0.859
11-1	1.174	1.149	1.519	0.998	1.193	1.61	1.087	1.253	1.112	1.024	0.911	0.793	1.263	0.868	0.833
11-2	1.165	1.138	1.508	0.986	1.178	1.594	1.076	1.24	1.1	1.015	0.903	0.782	1.253	0.859	0.824
11-3	1.068	1.062	1.386	0.936	1.127	1.491	1.009	1.16	1.042	0.947	0.842	0.754	1.156	0.809	0.777
12-1	1.17	1.137	1.513	0.979	1.166	1.592	1.072	1.238	1.092	1.013	0.902	0.769	1.257	0.855	0.821
12-2	1.097	1.081	1.422	0.944	1.133	1.515	1.024	1.179	1.052	0.964	0.857	0.756	1.183	0.819	0.787
12-3	1.076	1.054	1.393	0.916	1.097	1.477	0.998	1.15	1.022	0.94	0.836	0.73	1.158	0.797	0.765

Table 5 continued.

	$\varepsilon_{c\,Pre}/\varepsilon_{c\,Exp}$											
Specimen	[49]	[50]	[51]	[52]	[53]	[54]	[55]	[56]	[57] a	[57] b	[58]	[59]
1-1	1.332	1.104	0.939	1.171	1.629	1.034	0.876	1.151	0.892	0.806	1.018	0.799
1-2	1.383	1.146	0.975	1.213	1.692	1.087	0.91	1.195	0.926	0.837	1.057	0.831
1-3	1.364	1.131	0.962	1.203	1.667	1.047	0.897	1.179	0.913	0.825	1.042	0.818
2-1	1.377	1.142	0.97	1.25	1.671	0.928	0.902	1.196	0.921	0.83	1.052	0.818
2-2	1.389	1.151	0.979	1.232	1.695	1.04	0.912	1.201	0.93	0.839	1.061	0.831
2-3	1.443	1.196	1.017	1.291	1.757	1.04	0.947	1.25	0.966	0.871	1.102	0.861
3-1	1.413	1.173	0.995	1.32	1.704	0.823	0.924	1.234	0.946	0.849	1.079	0.834
3-2	1.341	1.114	0.945	1.258	1.616	0.761	0.876	1.172	0.898	0.806	1.025	0.79
3-3	1.377	1.144	0.971	1.304	1.656	0.741	0.899	1.206	0.922	0.826	1.052	0.81
4-1	1.42	1.18	1.001	1.339	1.71	0.785	0.928	1.243	0.951	0.853	1.085	0.836
4-2	1.422	1.185	1.004	1.383	1.703	0.644	0.928	1.255	0.953	0.852	1.088	0.832
4-3	1.385	1.153	0.977	1.332	1.662	0.676	0.904	1.219	0.928	0.83	1.059	0.812
5-1	1.449	1.209	1.024	1.431	1.731	0.589	0.945	1.285	0.972	0.868	1.11	0.846
5-2	1.418	1.179	1	1.351	1.704	0.735	0.926	1.244	0.949	0.851	1.084	0.833
5-3	1.459	1.215	1.029	1.415	1.748	0.675	0.952	1.287	0.978	0.874	1.116	0.854
6-1	1.41	1.178	0.997	1.399	1.683	0.551	0.92	1.252	0.947	0.844	1.081	0.823
6-2	1.414	1.178	0.998	1.375	1.693	0.64	0.922	1.248	0.948	0.847	1.082	0.828

	$\varepsilon_{c\,Pre}/\varepsilon_{c\,Exp}$											
Specimen	[49]	[50]	[51]	[52]	[53]	[54]	[55]	[56]	[57] a	[57] b	[58]	[59]
6-3	1.419	1.185	1.002	1.408	1.693	0.555	0.925	1.26	0.952	0.849	1.087	0.828
7-1	1.394	1.17	0.988	1.439	1.654	0.373	0.909	1.255	0.939	0.834	1.072	0.811
7-2	1.36	1.138	0.962	1.375	1.618	0.453	0.886	1.215	0.914	0.814	1.044	0.792
7-3	1.376	1.158	0.978	1.445	1.63	0.3	0.898	1.248	0.929	0.824	1.061	0.8
8-1	1.428	1.212	1.021	1.571	1.685	0.112	0.933	1.321	0.97	0.856	1.108	0.831
8-2	1.295	1.101	0.927	1.436	1.527	0.07	0.847	1.203	0.881	0.776	1.006	0.753
8-3	1.258	1.062	0.896	1.348	1.486	0.195	0.821	1.15	0.851	0.753	0.972	0.731
9-1	1.251	1.09	0.914	1.531	1.472	0.28	0.828	1.225	0.868	0.757	0.993	0.739
9-2	1.214	1.067	0.894	1.527	1.431	0.362	0.807	1.209	0.849	0.738	0.971	0.722
9-3	1.27	1.1	0.923	1.516	1.495	0.194	0.838	1.226	0.877	0.767	1.002	0.747
10-1	1.194	1.047	0.877	1.489	1.407	0.329	0.793	1.183	0.833	0.725	0.953	0.709
10-2	1.279	1.14	0.953	1.677	1.512	0.523	0.858	1.307	0.905	0.784	1.035	0.771
10-3	1.265	1.113	0.932	1.595	1.491	0.386	0.841	1.261	0.885	0.77	1.012	0.753
11-1	1.193	1.087	0.906	1.666	1.419	0.687	0.812	1.273	0.861	0.741	0.985	0.736
11-2	1.178	1.076	0.897	1.656	1.402	0.701	0.803	1.263	0.852	0.733	0.975	0.729
11-3	1.127	1.009	0.843	1.501	1.334	0.508	0.758	1.164	0.801	0.693	0.916	0.683
12-1	1.166	1.072	0.893	1.67	1.391	0.751	0.798	1.266	0.848	0.729	0.971	0.727
12-2	1.133	1.024	0.855	1.551	1.344	0.595	0.767	1.192	0.812	0.7	0.929	0.693
12-3	1.097	0.998	0.832	1.525	1.304	0.622	0.745	1.167	0.79	0.681	0.904	0.675

Table 5 continued.

	$\varepsilon_{c\,Pre}/\varepsilon_{c\,Exp}$											
Specimen	[60]	[61]	[62]	[63]	[64]	[65]	[66] a	[66] b	[66] c	[67]	[68]	Proposed
1-1	1.258	1.155	1.097	1.175	1.124	0.784	1.092	0.914	0.793	4.362	2.518	0.945
1-2	1.304	1.199	1.141	1.219	1.167	0.816	1.133	1.133	0.824	4.545	2.58	0.981
1-3	1.29	1.184	1.122	1.205	1.152	0.802	1.119	1.119	0.811	4.453	2.614	0.969
2-1	1.323	1.201	1.12	1.232	1.168	0.796	1.138	1.138	0.81	4.344	3.027	0.986
2-2	1.317	1.207	1.14	1.229	1.174	0.814	1.141	1.141	0.824	4.503	2.733	0.988
2-3	1.375	1.256	1.181	1.283	1.221	0.842	1.188	1.188	0.853	4.632	2.958	1.029
3-1	1.38	1.24	1.139	1.282	1.206	0.805	1.176	1.176	0.822	4.311	3.567	1.02
3-2	1.314	1.178	1.079	1.22	1.146	0.762	1.118	1.118	0.779	4.071	3.464	0.97
3-3	1.356	1.212	1.105	1.258	1.179	0.778	1.151	1.151	0.798	4.134	3.723	0.999

	$\varepsilon_{c\,Pre}/\varepsilon_{c\,Exp}$											
Specimen	[60]	[61]	[62]	[63]	[64]	[65]	[66] a	[66] b	[66] c	[67]	[68]	Proposed
4-1	1.395	1.249	1.141	1.295	1.215	0.805	1.186	1.186	0.824	4.287	3.753	1.029
4-2	1.425	1.261	1.133	1.319	1.226	0.792	1.199	1.199	0.816	4.138	4.402	1.042
4-3	1.378	1.224	1.107	1.277	1.191	0.776	1.164	1.164	0.798	4.084	4.052	1.011
5-1	1.467	1.29	1.151	1.356	1.255	0.801	1.228	1.228	0.828	4.146	4.835	1.068
5-2	1.402	1.25	1.136	1.3	1.216	0.799	1.188	1.188	0.82	4.226	3.955	1.031
5-3	1.459	1.292	1.163	1.351	1.257	0.814	1.229	1.229	0.838	4.262	4.443	1.068
6-1	1.432	1.257	1.119	1.324	1.223	0.778	1.198	1.198	0.805	4.012	4.827	1.041
6-2	1.417	1.253	1.126	1.312	1.219	0.788	1.192	1.192	0.812	4.115	4.377	1.036
6-3	1.441	1.265	1.125	1.331	1.23	0.782	1.205	1.205	0.809	4.036	4.855	1.047
7-1	1.455	1.257	1.098	1.341	1.224	0.753	1.201	1.201	0.786	3.791	5.852	1.046
7-2	1.399	1.219	1.074	1.291	1.186	0.743	1.162	1.162	0.771	3.787	5.12	1.011
7-3	1.454	1.248	1.082	1.338	1.216	0.738	1.194	1.194	0.773	3.676	6.292	1.04
8-1	1.563	1.316	1.118	1.433	1.285	0.749	1.263	1.263	0.793	3.626	8.315	1.102
8-2	1.426	1.197	1.014	1.307	1.169	0.677	1.149	1.149	0.717	3.259	7.869	1.004
8-3	1.35	1.149	0.986	1.24	1.12	0.668	1.1	1.1	0.702	3.282	6.404	0.959
9-1	1.491	1.204	0.987	1.359	1.184	0.629	1.164	1.164	0.682	2.86	12.54	1.02
9-2	1.481	1.184	0.962	1.347	1.166	0.605	1.146	1.146	0.66	2.71	13.95	1.005
9-3	1.483	1.21	0.999	1.353	1.187	0.645	1.167	1.167	0.695	2.975	11.2	1.022
10-1	1.447	1.16	0.945	1.316	1.141	0.597	1.122	1.122	0.65	2.685	13.16	0.984
10-2	1.617	1.272	1.024	1.468	1.257	0.629	1.234	1.234	0.693	2.758	18.02	1.085
10-3	1.547	1.235	1.003	1.407	1.216	0.63	1.195	1.195	0.687	2.816	14.74	1.049
11-1	1.594	1.225	0.973	1.443	1.218	0.577	1.193	1.193	0.646	2.449	22.8	1.05
11-2	1.583	1.213	0.963	1.433	1.207	0.569	1.182	1.182	0.637	2.404	23.29	1.041
11-3	1.444	1.13	0.906	1.31	1.118	0.552	1.097	1.097	0.611	2.399	17.14	0.964
12-1	1.593	1.213	0.959	1.441	1.209	0.56	1.183	1.183	0.631	2.348	25.17	1.043
12-2	1.487	1.151	0.918	1.348	1.142	0.551	1.12	1.12	0.613	2.358	19.74	0.986
12-3	1.46	1.124	0.893	1.322	1.117	0.531	1.094	1.094	0.593	2.257	20.6	0.963

When R^2 equals the value of one that does not mean a perfect prediction because other indices influence the selection. In Table 6, the predictions of two strain models [36, 62] yielded equal values of R^2 (0.736) but with higher values of AAE (9.4% and 9.02%) and lower values of E1 (0.99 and 0.988) compared with 3.46% and 0.998 for the proposed model. Therefore, for this kind of evaluation, R^2 is not the most critical index.

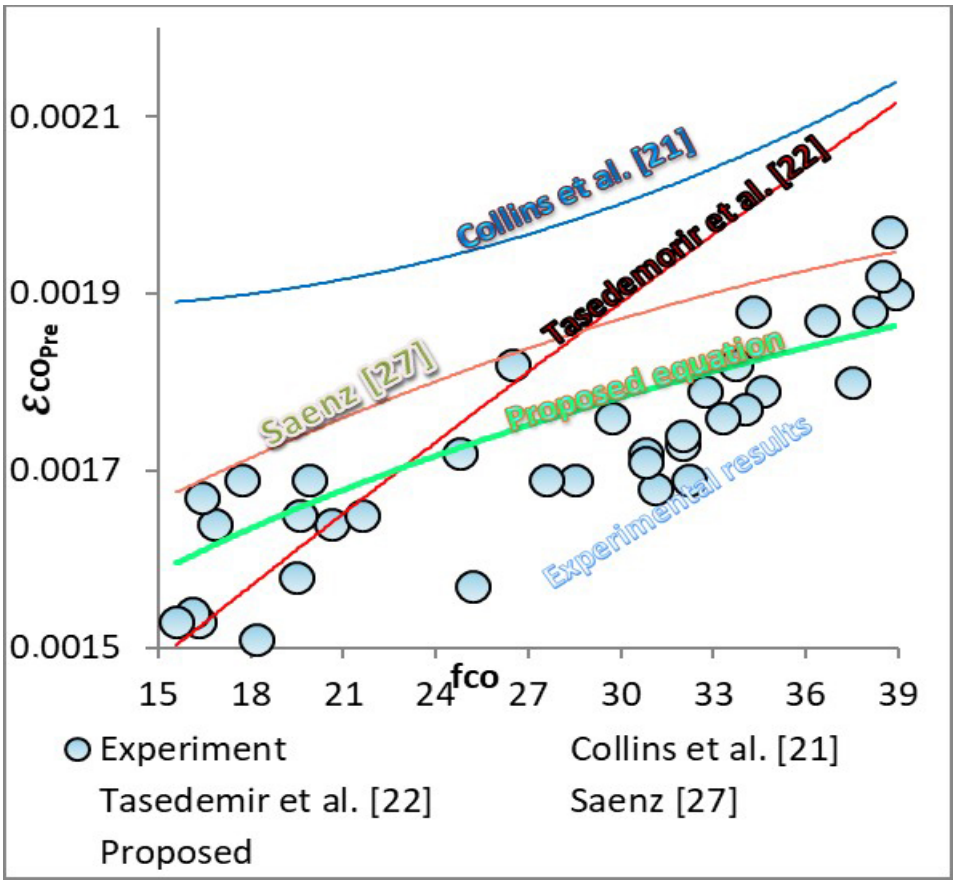

Figure. 7. Predicted strain at peak stress versus the f_c for G-1 strain models with polynomial functions.

3.6. Applicability of strain models

The five best performing models [27, 33, 44, 51, 58] and the proposed ANN-based model were checked against the test results reported by Woldemariam et al. [77] for concrete strain at peak stress, specimens C1 (ε_c =0.0021), C2 (ε_c =0.0026), C3 (ε_c =0.0029), C4 (ε_c =0.0031), C5 (ε_c =0.0033), respectively. The values of AAE in percentage were 38.7 [27], 39.6 [33], 43.21 [44], 49.7 [58], and 41.5 for the proposed model, respectively. The corresponding values of NRMSE were close, 0.021 [27], 0.022 [33], 0.021 [44], 0.026 [58], and 0.022 for the proposed model, respectively. However, it was slightly higher for model [51] with a value of 0.026, (Fig. 11). For the coefficient of correlation, the corresponding values were (0.985, 0.945, 0.98, 0.992, 0.992) for the five models [27, 33, 44, 51, 58] and 0.988 for the proposed model. However, other statistical measures show more measured errors (standard deviations with values of 0.07, 0.102, 0.052, 0.034, and 0.037 for the five models and 0.068 for the proposed model), Fig. 11.

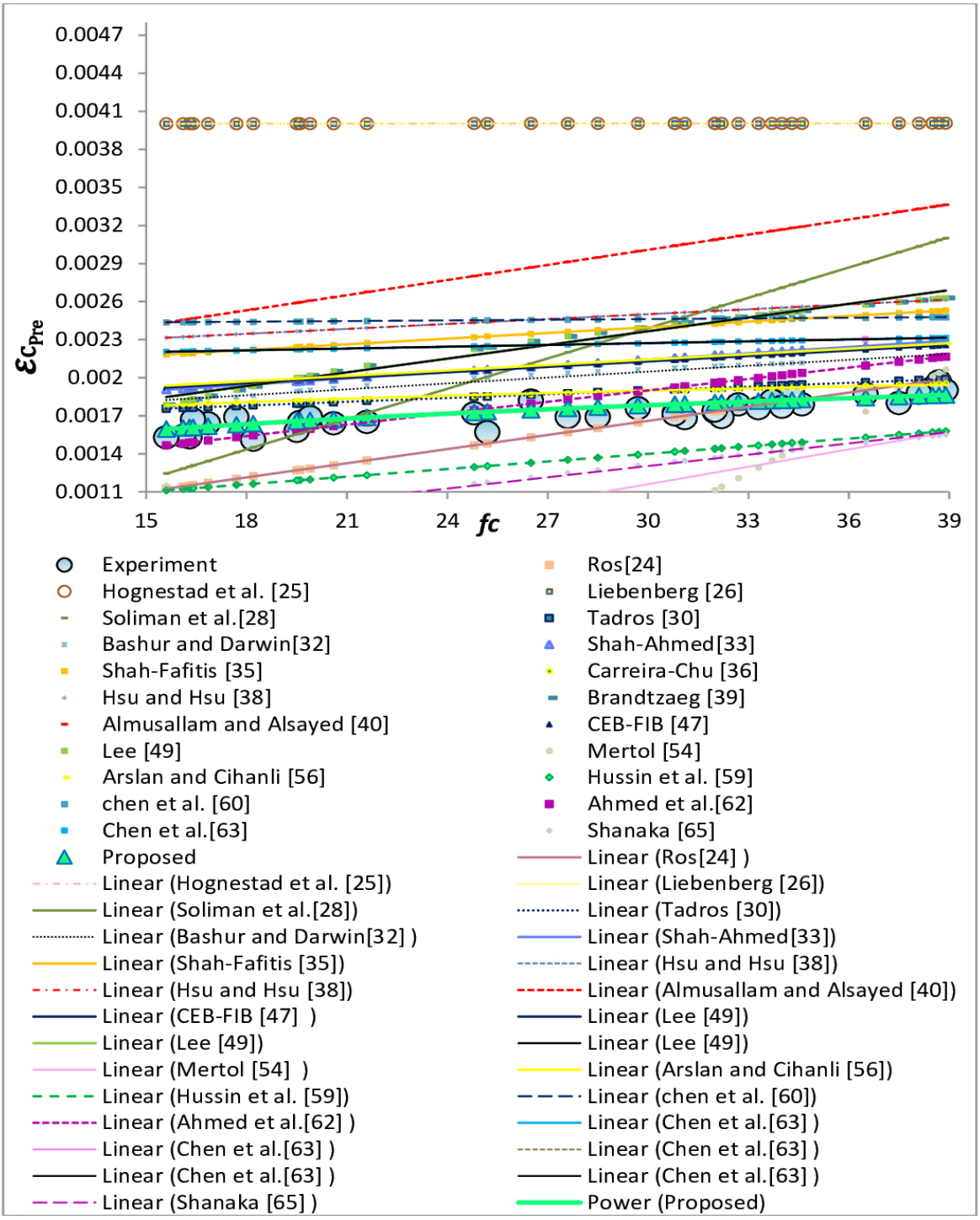

Figure. 8. Predicted strain at peak stress versus the f_c for G-2 strain models with linear functions.

The corresponding values of covariance are 0.005, 0.01, 0.003, 0.001, and 0.0014 for the five models [27, 33, 44, 51, 58] and 0.004 for the proposed model, respectively. Therefore the efficiency of the models in predicting the strain at peak stress can be better represented by the four indexes AAE, NRMSE, E, and E1 compared with the R^2 index.

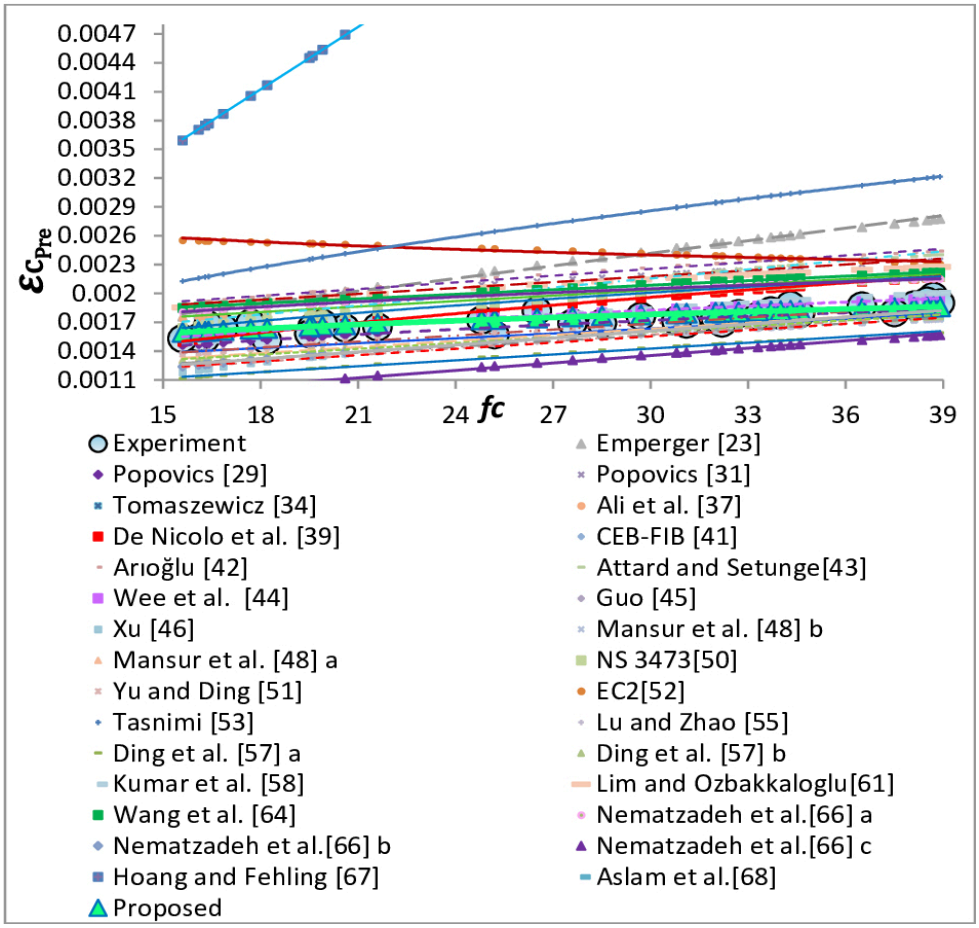

Figure. 9. Predicted strain at peak stress versus the f_c for G-3 strain models with power functions.

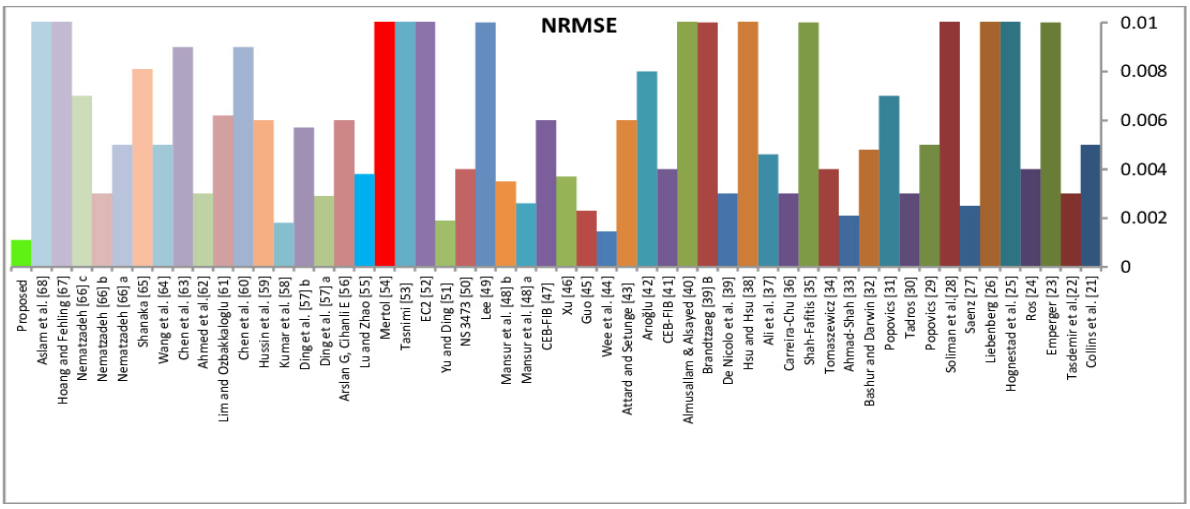

Figure 10. NRMSE values in model predictions of strain at peak stress [21-68] and the proposed model.

Table 6. Performance of the strain models using statistical indexes.

Model	*Min.*	*Max.*	*Mean*	*COV*	*STD*	*NRMSE*	*AAE(%)*	*E*	*E1*	R^2
Collins et al. [21]	1.077	1.255	1.161	0.002	0.045	0.005	16.09	0.973	0.837	0.744
Tasdemir et al.[22]	0.913	1.156	1.060	0.005	0.069	0.003	7.85	0.991	0.918	0.732
Emperger [23]	1.079	1.514	1.343	0.017	0.131	0.010	34.33	0.854	0.642	0.720
Ros [24]	0.929	1.446	1.118	0.025	0.158	0.004	10.70	0.980	0.894	0.736
Hognestad et al. [25]	2.033	2.651	2.336	0.024	0.157	0.037	133.6	-0.818	-0.36	0.706
Liebenberg [26]	2.034	2.651	2.336	0.024	0.157	0.037	133.6	-0.818	-0.36	0.706
Saenz [27]	0.988	1.158	1.067	0.002	0.040	0.0025	6.761	0.994	0.932	0.701

Model	*Min.*	*Max.*	*Mean*	*COV*	*STD*	*NRMSE*	*AAE(%)*	*E*	*E1*	R^2
Soliman et al.[28]	0.783	1.660	1.271	0.083	0.290	0.0110	34.02	0.823	0.64	0.736
Popovics [29]	1.054	1.249	1.158	0.002	0.047	0.005	15.79	0.972	0.838	0.711
Tadros [30]	1.009	1.18	1.093	0.002	0.042	0.003	9.29	0.99	0.907	0.736
Popovics [31]	1.129	1.337	1.24	0.002	0.050	0.007	24.00	0.938	0.735	0.711
Bashur and Darwin [32]	1.084	1.276	1.171	0.002	0.045	0.0048	17.10	0.968	0.826	0.675
Ahmad-Shah [33]	0.839	1.093	0.963	0.004	0.064	0.0021	6.08	0.994	0.936	0.736
Tomaszewicz [34]	0.998	1.215	1.129	0.003	0.058	0.004	12.87	0.979	0.867	0.713
Shah-Fafitis [35]	1.283	1.481	1.375	0.002	0.049	0.01	37.53	0.855	0.616	0.736
Carreira-Chu [36]	0.992	1.198	1.093	0.002	0.049	0.003	9.37	0.99	0.907	0.736
Ali et al. [37]	1.054	1.249	1.158	0.002	0.047	0.0046	15.8	0.972	0.834	0.711
Hsu and Hsu [38]	1.327	1.555	1.439	0.003	0.056	0.0121	43.9	0.803	0.522	0.736
De Nicolo et al. [39]	0.916	1.194	1.09	0.006	0.08	0.003	10.44	0.984	0.891	0.714
Brandtzaeg [39] B	1.097	1.459	1.325	0.011	0.104	0.01	32.47	0.876	0.663	0.693
Almusallam & Alsayed [40]	1.477	1.837	1.694	0.01	0.101	0.02	69.35	0.484	0.284	0.736
CEB-FIB [41]	0.998	1.215	1.129	0.003	0.058	0.004	12.87	0.979	0.867	0.713
Arıoğlu [42]	1.15	1.378	1.28	0.003	0.057	0.008	27.97	0.915	0.712	0.712.
Attard and Setunge [43]	1.022	1.324	1.21	0.007	0.086	0.006	20.99	0.945	0.781	0.711
Wee et al. [44]	0.94	1.113	1.032	0.002	0.042	0.001	4.45	0.997	0.955	0.711
Guo [45]	0.836	0.996	0.927	0.002	0.041	0.0023	7.24	0.993	0.925	0.72
Xu [46]	0.73	0.967	0.88	.0045	0.068	0.0037	11.95	0.982	0.879	0.697
CEB-FIB [47]	1.142	1.312	1.22	0.002	0.043	0.006	21.96	0.95	0.776	0.736
Mansur et al. [48] a	0.797	0.997	0.92	0.003	0.055	0.0026	8.04	0.991	0.919	0.715
Mansur et al. [48] b	0.765	0.957	0.883	0.003	0.053	0.0035	11.71	0.984	0.881	0.715
Lee [49]	1.097	1.459	1.325	0.011	0.104	0.01	32.47	0.876	0.663	0.693
NS 3473 [50]	0.998	1.215	1.129	0.003	0.058	0.004	12.87	0.979	0.867	0.713
Yu and Ding [51]	0.832	1.029	0.952	0.0028	0.053	0.0019	5.34	0.995	0.946	0.714
EC2 [52]	1.171	1.677	1.422	0.019	0.139	0.012	42.20	0.812	0.575	0.755
Tasnimi [53]	1.304	1.757	1.584	0.018	0.134	0.017	58.38	0.618	0.395	0.718
Mertol [54]	0.072	1.087	0.605	0.073	0.727	0.013	40.85	0.775	0.589	0.436
Lu and Zhao [55]	0.745	0.952	0.873	0.0033	0.058	0.0038	12.69	0.981	0.871	0.716
Arslan G, Cihanli E [56]	1.15	1.321	1.228	0.002	0.043	0.006	22.79	0.946	0.767	0.736
Ding et al. [57] a	0.79	0.978	0.904	0.0025	0.051	0.0029	9.57	0.988	0.903	0.714
Ding et al. [57] b	0.68	0.874	0.801	0.003	0.055	0.0057	19.92	0.957	0.797	0.716
Kumar et al. [58]	0.904	1.117	1.033	0.0032	0.057	0.0018	5.71	0.995	0.941	0.714
Hussin et al. [59]	0.675	0.861	0.786	0.003	0.053	0.006	21.43	0.951	0.781	0.736
Chen et al. [60]	1.175	1.468	1.318	0.005	0.071	0.009	31.84	0.896	0.677	0.736
Lim and Ozbakkaloglu [61]	1.123	1.316	1.219	0.0021	0.046	0.0062	21.89	0.949	0.776	0.71
Ahmed et al.[62]	0.893	1.181	1.062	0.007	0.083	0.003	9.02	0.988	0.906	0.736
Chen et al. [63]	1.175	1.468	1.318	0.005	0.071	0.009	31.84	0.896	0.677	0.736
Wang et al. [64]	1.117	1.285	1.193	0.002	0.042	0.005	19.25	0.961	0.803	0.724
Shanaka [65]	0.531	0.842	0.715	0.0094	0.097	0.0081	28.51	0.912	0.711	0.722
Nematzadeh [66] a	1.091	1.2629	1.167	0.0017	0.042	0.005	16.7	0.97	0.83	0.709
Nematzadeh [66] b	0.757	0.9875	0.901	0.0044	0.067	0.003	9.88	0.986	0.901	0.717
Nematzadeh [66] c	0.593	0.8533	0.750	0.0061	0.079	0.007	24.99	0.932	0.746	0.721
Hoang and Fehling [67]	2.257	4.632	3.586	0.602	0.782	0.077	258.6	-6.96	-1.7	0.735
Aslam et al. [68]	2.518	25.17	8.858	47.28	6.924	0.27	785.8	-96.51	-6.71	0.598
Proposed	0.945	1.102	1.018	0.001	0.037	0.0011	3.46	0.998	0.965	0.708

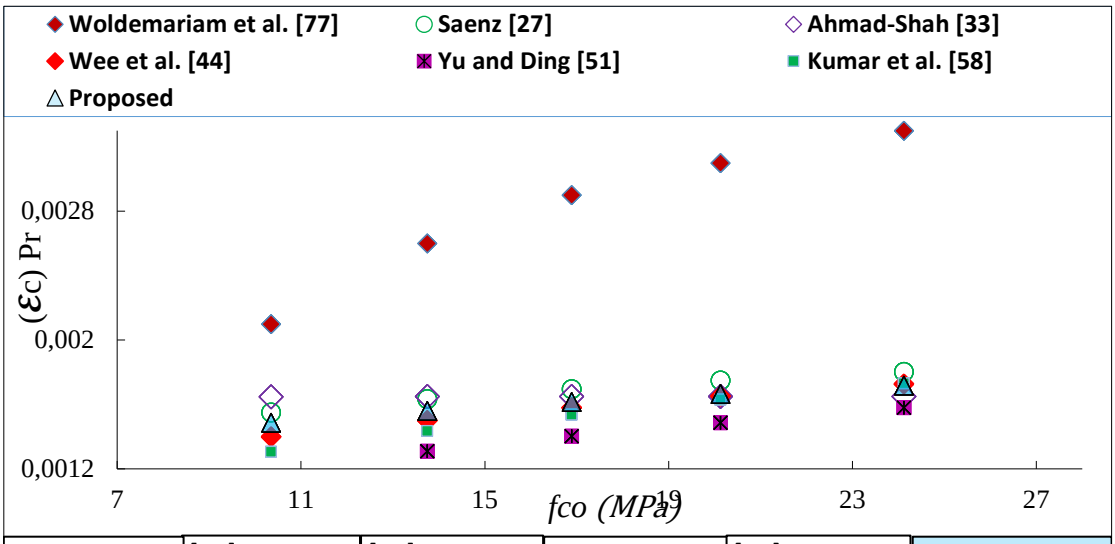

[27]	[33]	[44]	[51]	[58]	Proposed
NRMSE=0.021	NRMSE=0.022	NRMSE=0.021	NRMSE=0.026	NRMSE=0.023	NRMSE=0.022
AAE=38.7%	AAE=39.6%	AAE=43.21%	AAE=49.7%	AAE=44.9%	AAE=41.5%
E=0.828	E=0.78	E=0.795	E=0.737	E=0.784	E=0.804
E1=0.59	E1=0.58	E1=0.55	E1=0.54	E1=0.534	E1=0.56
R^2 =0.985	R^2 =0.945	R^2 =0.98	R^2 =0.992	R^2 =0.992	R^2 =0.988
STD=0.07	STD=0.102	STD=0.052	STD=0.034	STD=0.037	STD=0.068
COV=0.005	COV=0.01	COV=0.003	COV=0.001	COV=0.0014	COV=0.004

Figure 11. Strain predictions of test results of [77] using models [27, 33, 44, 51, 58] and the proposed model.

4. Conclusions

1. Several parameters such as aggregate/cement ratio, w/c ratio, and slump values that influence the compressive strength and strain at peak stress of concrete were considered as input for the two ANN models.

2. The developed ANN models successfully yielded good predictions of the test results presented in the current study.

3. The AAE value was found to be less than 3.46% for the proposed model, and the NRMSE value was the lowest, 0.0011.

4. The predicted strains obtained from the regression of ANN output data for stress and strain at peak stress were more accurate than those obtained from the fifty-three existing expressions for predicting the strain at peak stress.

5. Both the NRMSE and AAE indexes allow the assessing of the performance of the strain models for the present study more properly than the R^2 index. ANN procedure is a valuable modeling technique for practicing engineers interested in concrete technology.

6. The models with power function show better performance in predicting the strain at peak stress than models with linear or polynomial functions.

New research should be carried out along these lines to include input parameters outside the range considered in the present study and to improve the prediction capability of the proposed model and its application to test data with higher strengths.

References

1. Saridemir, M. Prediction of compressive strength of concretes containing metakaolin and silica fume by Artificial Neural Networks. Advances in Engineering Software. 2009. 40. Pp. 350–355. DOI: 10.1016/j.advengsoft.2008.05.002
2. Chopra, P., Sharma, R.K., Kumar, M. Prediction of compressive strength of concrete using artificial neural network and genetic programming. Advances in Materials Science and Engineering. 2016. ID 7648467. Pp. 1–10. DOI: 10.1155/2016/7648467
3. Lai, S., Serra, M. Concrete strength prediction neural network. Construction and Building Materials. 1997. 11(2). Pp. 93–98. DOI: 10.1016/S0950-0618(97)00007-X
4. Oztas, A., Pala, M., Ozbay, E., Kanca, E., Caglar, N., Bhatti, M. A. Predicting the compressive strength and slump of high strength concrete using neural network. Construction and Building Materials. 2016. 20. Pp. 769–775. DOI: 10. 1016/j. conbuildmat.2005.01.054
5. Naderpour, H., Mirrashid, M. An innovative approach for compressive strength estimation of mortars having calcium inosilicate minerals. Journal of Building Engineering. 2018. 19. Pp. 205–215. DOI: 10.1016/j.jobe.2018.05.012

6. Asteris, P.G., Kolovos, K.G., Douvika, M.G., Roinos, K. Prediction of self-compacting concrete strength using artificial neural networks. European Journal of Environmental and Civil Engineering. 2016. 20(1). Pp. 102–122.DOI: .org/10. 1080/19648189.2016.1246693
7. Duan, Z. H., Kou, S. C., Poon, C. S. Prediction of compressive strength of recycled aggregate concrete using artificial neural networks. Construction and Building Materials. 2013. 40. Pp. 1200–1206. DOI: 10.1016/j.conbuildmat.2012.04.063
8. Momeni, E., Armaghani, D. J., Hajihassani, M. Prediction of uniaxial compressive strength of rock samples using hybrid particle swarm optimization-based artificial neural networks. Measurement. 2015. 60. Pp. 50–63. DOI: 10.1016/j.measurement.2014.09.075
9. Ahmad, A., Kotsovou, G., Cotsovos, D.M., Lagaros, N.D. Assessing the accuracy of RC design code predictions through the use of artificial neural networks. International Journal of Advanced Structural Engineering. 2018. 10(4). Pp. 349–365. DOI: 10.1007/s40091-018-0202-4
10. Charhate, S., Subhedar, M., Adsul, N. Prediction of Concrete Properties Using Multiple Linear Regression and Artificial Neural Network. Journal of Soft Computing in Civil Engineering. 2018. 2-3. Pp. 27–3. DOI: 10.22115/scce.2018.112140.1041
11. Pala, M., Ozbay, E., Oztas, A., Yuce, M. I. Appraisal of long-term effects of fly ash and silica fume on compressive strength of concrete by neural networks. Construction and Building Materials. 2007. 21(2). Pp. 384–394.DOI: 10.1016/j. conbuildmat.2005.08.009
12. Svozil, D., Kvasnicka, V., Pospichal, J. Introduction to multi-layer feed-forward neural networks. Chemometrics and Intelligent Laboratory Systems. 1997. 39. Pp. 43–62.
13. Basher, I.A., Hajmeer, M. Artificial neural networks: fundamentals, computing, design, and application. Journal of Microbial Methods. 2000. 43. Pp. 3–31. DOI: 10.1016/s0167-7012(00)00201-3
14. Abdulla, N.A. Concrete encased with engineering plastics. Journal of Civil Engineering and Construction. 2020. 9 (1). Pp. 31–41. DOI: 10.32732/jcec.2020.9.1.31
15. Adhikary, B.B., Mutsuyoshi, H. Prediction of shear strength of steel fiber RC beams using neural networks. Construction and Building Materials. 2006. 20(9). Pp. 801–11. DOI:10.1016/j.conbuildmat.2005.01.047
16. Nikbin, I.M., Rahimi, S., Allahyari, H. A new empirical formula for prediction of fracture energy of concrete based on the artificial neural network. Engineering Fracture Mechanics. 2017. 186. Pp.466–82.DOI: 10.1016/j.engfracmech.2017.11.010
17. Naderpour, H., Kheyroddin, A., Amiri, G.G. Prediction of FRP-confined compressive strength of concrete using artificial neural networks. Composite Structures. 2010. 92. Pp. 2817–29. DOI: 10.1016/j.compstruct.2010.04.008
18. Kassem, A. A., Raheem, A. M., Khidir, K. M., Alkattan, M. Predicting of daily Khazir basin flow using SWAT and hybrid SWAT-ANN Models. Ain Shams Engineering Journal. 2019. DOI: 10.1016/j.asej.2019.10.011
19. Demir, F. Prediction of elastic modulus of normal and high strength concrete by artificial neural networks. Construction and Building Materials. 2008. 22(7). Pp. 1428–1435. DOI: 10.1016/j.conbuildmat.2007.04.004
20. Maghreb, M., Sammut, C., Waller, T. Predicting the duration of concrete operations via artificial neural network and by focusing on supply chain parameters. Building Research Journal. 2014. 61(1). Pp. 1–14. DOI: 10.2478/brj-2014-0001
21. Collins, P.M., Mitchell, D., Macgregor, J.G. Structural design considerations for high-strength concrete. Concrete International. 1993. Pp. 27-34.
22. Tasdemir, M., Tasdemir, C., Akyüz, S., Jefferson, A., Lydon, F., Barr, B., Evaluation of strains at peak stresses in concrete: a three-phase composite model approach. Cement and Concrete Composites. 1998. 20 (4). Pp. 301–318. DOI: 10.1016/S0958-9465(98)00012-2
23. Emperger, F.V. Der Beiwert n. Beton und Eisen. 1936. 35(19). Pp. 324–332.
24. Ros, M. Material-technological foundation and problems of reinforced concrete. Bericht No. 162 (Eidgenossische Material prfifungs und Versuchs anstalt f/Jr Industrie, Bauwesen and Gewerbe, Zurich, Switzerland 1950.
25. Hognestad, E., Hanson, N.W., Mchenry, D. Concrete stress distribution in ultimate strength design. Journal of the American Concrete Institute. 1955. 27 (4). Pp. 455–479.
26. Liebenberg, A.C. A stress-strain function for concrete subjected to short-term loading, Magazine of concrete Research. 1962. 14. Pp. 85–99.
27. Saenz, L.P. Discussion of a paper by Desayi P, Krishnan S. Equation for the stress-strain curve of concrete. Ibid. 1964. 61(9). Pp. 1229–1235.
28. Soliman, M.T.M. The flexural stress-strain relationship of concrete confined by rectangular transverse reinforcement, Magazine of Concrete Research. 1967. 19(61). Pp. 223–238. DOI: 10.1680/macr.1967.19.61.223
29. Popovics, S. A review of stress-strain relationships for concrete. ACI Journal. 1970. 67(3). Pp. 243-248.
30. Tadros, G.S. Plastic rotation of reinforced concrete members subjected to bending, axial load, and shear. Ph.D. Thesis, University of Calgary. 1970.
31. Popovics, S. A numerical approach to the complete Stress-strain curve of concrete, Cement, and Concrete Research. 1973. 3. Pp. 583–599
32. Fuad K. Bashur David Darwin. Nonlinear model for reinforced concrete slabs. A Report on a Research Project Sponsored by THE National Science Foundation Research Grant Eng76-09444 University of Kansas Lawrence, Kansas December 1976
33. Ahmad, S.H., Shah, S.P. Behavior of hoop confined concrete under high strain rates. ACI Journal. 1982. 82. Pp. 634–647.
34. Tomaszewicz, A. Betongens Arbeidsdiagram: SINTEF Rep. No. STF 65A84605, Trondheim. 1984.
35. Shah, S.P., Fafitis, A. Predictions of ultimate behavior of confined columns subjected to large deformations. Ibid. 1985. 82(4). Pp. 423–433.
36. Carreira, D.J., Chu, K. H. Stress-Strain relationship for plain concrete in compression. Journal of American Concrete Institute. 1986. 82(6). Pp. 797–804
37. Ali AM, Farid BJ, Al-Janabi AJM. Stress-strain relationship for concrete in compression made of local materials. Engineering Science. 1990. 2(1). Pp. 183–194
38. Hsu LS, Hsu CT. Complete stress-strain behavior of high-strength concrete under compression. Magazine of Concrete Research. 1994. 46(169). Pp. 301–12
39. De Nicolo, B., Pani, L., Pozzo, E. Strain of concrete at peak compressive stress for a wide range of compressive strengths. Materials and Structures**.** 1994. 27(4). Pp. 206–210. DOI: org/10.1007/BF02473034
40. Al Musallam, T. H., Al Sayed, S. H. Stress-strain relationship of normal, high, and lightweight concrete. Magazine of Concrete Research. 1995. 47(170). Pp. 39–44. DOI: https://doi.org/10.1680/macr.1995.47.170.39

41. CEB-FIB. High-Performance Concrete-Recommended Extensions to the Model code 90, Research Needs. International Federation for Structural Concrete (fib), Lausanne, Switzerland. 1995.
42. Arıoğlu, E. Strain of Concrete at Peak Compressive Stress for a Wide Range of Compressive Strengths. Discussion on paper by B. de Nicolo, L. Panni, E. Pozzo, Materials and Structures, RILEM. 1995. 28(184). Pp. 611–614
43. Attard M. M., Setunge, S. Stress-strain relationship of confined and unconfined concrete. ACI Materials journal.1996. 93(5). Pp. 432–442
44. Wee, T.H., Chin, M.S., Mansur, M.A. Stress-strain relationship of high-strength Concrete in compression. Journal of Materials in Civil Engineering. 1996. 8(12). Pp. 70–76. DOI: 10.1061/(ASCE)0899-1561(1996)8:2(70)
45. Guo, Z.H. Strength and deformation of concrete (test foundation and constitutive relationship). Beijing: Tsinghua University Press, China. 1997 (in Chinese)
46. Xu, L.Y. Experimental research on stress-strain curves of high-performance concrete and compact, reinforced high-performance concrete in tension. Dissertation for the Doctoral Degree. Wuhan: Wuhan University of Hydraulic and Electric Engineering. 1998 (in Chinese)
47. CEB-FIB. Structural Concrete-Textbook on behavior, design, and performances (Updated knowledge of CEB/FIP Model Code 1990), International Federation for Structural Concrete (fib), Lausanne, Switzerland. 1990.
48. Mansur M.A., Chin M. S., Wee T. H. Stress-strain relationship of confined high strength plain and fiber concrete– closure. Journal of Materials in Civil Engineering. 1999. 11(4). Pp. 364-364.
49. Lee, I. Complete stress-strain characteristics of high-performance concrete Ph.D. thesis. New Jersey Institute of Technology. 2002.
50. NS 3473. Concrete structures-design and detailing rules. Norwegian Standards. 2003.
51. Yu, Z. W., Ding, F. X. Calculation method of compressive mechanical properties of concrete. Journal Building Structures. 2003. 24(4). Pp. 41–46 (In Chinese)
52. Euro code. Design of concrete structures–Part 1-1: General rules and rules for building. European Committee for Standardization (CEN), Brussels, Belgium. 2004.
53. Tasnimi, A.A. Mathematical model for complete stress-strain curve prediction of normal, lightweight, and high-strength concretes. Magazine of Concrete Research. 2004. 56(1). Pp. 23-34. DOI: 10.1680/macr.2004.56.1.23
54. Mertol, H.C. Behavior of high-strength concrete members subjected to combined flexure and axial compression loadings. Ph.D. thesis. Raleigh, North Carolina. 2006.
55. Lu Z. H., Zhao, Y.G. An improved analytical constitutive relation for normal weight high-strength concrete. International Journal of Modern Physics B. 2008. 22(31–32). Pp. 5425–30.
56. Arslan, G., Cihanli, E. Curvature ductility prediction of reinforced high-strength concrete beam sections. Journal of Civil Engineering and Management. 2010. 16(4). Pp. 462–470. DOI: doi.org/10.3846/jcem.2010.52
57. Ding, F., Ying, X., Zhou, L., Yu Z. Unified calculation method, and its application in determining the uniaxial mechanical properties of concrete. Frontiers in Architectural and Civil Engineering. 2011. 5(3). Pp. 381–393. DOI 10.1007/s11709-011-0118-6
58. Kumar R., Singh, B., Bhargava, P. Flexural capacity predictions of SCC beams using stress-strain relationship in axial compression. Magazine of Concrete Research. 2011. 63(1). Pp. 49–59. DOI: 10.1680/macr.2011.63.1.49
59. Hussin, M., Zhuge, Y., Bullen, F., Lokuge, W. A mathematical model for complete stress-strain curve prediction of permeable concrete. Proceedings of the 22nd Australasian Conference on the Mechanics of Structures and Materials (ACMSM 22). Taylor & Francis (CRC Press) / Balkema. 2013. Pp. 293-298.
60. Chen, Y., Visintin, P., Oehlers, D. J. Mechanism orientated stress-strain model for unconfined concrete. Departmental Rep. R-181, School of Civil, Environmental and Mining Engineering University of Adelaide, SA, Australia. 2013.
61. Lim, J.C., Ozbakkaloglu, T. Stress–strain model for normal- and lightweight concretes under uniaxial and triaxial compression. Construction and Building Materials. 2014. 71. Pp. 492–509
62. Ahmad, S., Pilakoutas, K., Khan, Q.Z, Neocleous, K. Stress-Strain Model for Low-Strength Concrete in Uni-Axial Compression. Arabian Journal of Science and Engineering. 2015. 40**.** Pp. 313–328. https://doi.org/10.1007/s13369-014-1411-1
63. Chen, Y., Visintin, P., Oehlers, D.J., Alengaram, U.J. Size-Dependent Stress-Strain Model for Unconfined Concrete. Journal of Structural Engineering. 2015. 140. DOI: 10.1061/(ASCE)ST.1943-541X.0000869
64. Wang, Z., Wang, J., Liu, T., Zhang, F. Modeling seismic performance of high strength steel-ultra-high-performance concrete piers with modified Kent-Park model using fiber elements. Advanced Mechanical Engineering. 2016. 8(2). Pp.1–13. DOI: 10.1177/1687814016633411
65. Shanaka, K. Ductility Design of Very-High Strength Reinforced Concrete Columns (100–150 MPa). Ph.D. thesis. The University of Melbourne. 2016
66. Nematzadeh, M., Salari, A., Ghadami, J., Naghipour, M. Stress-strain behavior of freshly compressed concrete under axial compression with a practical equation. Construction and Building Materials. 2016. 115. Pp. 402–423. DOI: 10.1016/j.conbuildmat.2016.04.045
67. Hoang, A.L., Fehling, E. Influence of steel fiber content and aspect ratio on the uniaxial tensile and compressive behavior of ultra-high-performance concrete. Construction and Building Materials. 2017. 153. Pp. 790–806. DOI: 10.1016/j.conbuildmat.2017.07.130
68. Aslam, M., Shafigh, P., Nomeli, M.A., Jumaat, M.Z. Manufacturing of high-strength lightweight aggregate concrete using blended coarse lightweight aggregates. Journal of building Engineering. 2017. 13. Pp. 53-62. DOI: 10.1016/j.conbuildmat.2017.07.130
69. CEB-FIP Model Code 1990 *//* Bulletin d'lnformation No. 203, Chap. 2. 1991.
70. Z. Guo, X. Zhang. Investigation of complete stress-deformation curves for concrete in tension. ACI Materials Journal. 1987. 84. Pp. 278–285
71. Sargin, M., Ghosh, S.K. Handa, V.K. Effects of lateral reinforcement upon the strength and deformation properties of concrete. Magazine of Concrete Research. 1971. 23 (75–76). Pp. 99–110
72. Xie, N., Liu, W. Determining tensile properties of mass concrete by direct tensile test. ACI Materials journal. 1989. 86. Pp. 214–219
73. Phillips, D.V. Zhang, B. Direct tension tests on notched and unnotched plain concrete specimens. Magazine of concrete research. 1993. 45. Pp. 25–35
74. Kaklauskas, G. Practical techniques for determining of Average stress-strain relationships for concrete from experimental data Of RC bending members. Statyba. 1998. 4(1). Pp. 20-28, DOI: 10.1080/13921525. 1998.10531375
75. Jensen, V. P. The Plasticity Ratio of Concrete and Its Effect on the Ultimate Strength of Beams. Journal of the American Concrete Institute. 1943. 14(6). Pp. 565-582

76. Thorenfeldt, E., Tomaszewicz, A., Jensen, J. J. Mechanical Properties of High-Strength Concrete and Application in Design. Proceedings of Utilization of High Strength Concrete Symposium, Stavanger, Norway. 1987. Pp. 149–159
77. Woldemariam, A. M., Oyawa, W. O., Nyomboi, T. Structural performance of UPVC confined concrete equivalent cylinders under axial compression loads. Buildings. 2019. 9(4). Pp. 82. DOI: 10.3390/buildings9040082.

Contacts:

Nwzad Abduljabar Abdulla, anwzad@yahoo.com

Received 27.05.2020. Approved after reviewing 11.05.2021. Accepted 12.05.2021.